Per. Mineral. (2007), 76, 127-153
SPECIAL ISSUE: In honour of Ezio Callegari on his retirement
doi:10.2451/2007PM0021
http://go.to/permin

PERIODICO di MINERALOGIA
established in 1930

An International Journal of
MINERALOGY, CRYSTALLOGRAPHY, GEOCHEMISTRY, ORE DEPOSITS, PETROLOGY, VOLCANOLOGY
and applied topics on *Environment*, *Archaeometry* and *Cultural Heritage*

Metamorphic veins from the serpentinites of the Piemonte Zone, western Alps, Italy: a review

CHIARA GROPPO [1, 2*] and ROBERTO COMPAGNONI [1, 2]

[1] Dipartimento di Scienze Mineralogiche e Petrologiche, Università degli Studi di Torino,Via Valperga Caluso, 35, 10125 Torino, Italy
[2] Centro interdipartimentale "G. Scansetti" per lo studio sull' Asbesto e altri particolati tossici, Università degli Studi di Torino, Italy

ABSTRACT. — Petrographic and micro-Raman analysis of metamorphic veins occurring in serpentinites from the Piemonte Zone (western Alps) has allowed us to recognise seven different vein generations, developed at different *P-T-X* conditions. The first vein generation (balangeroite + magnetite + FeNi-alloys) formed during the Alpine prograde evolution, whereas the second vein generation (diopside + Ti-clinohumite + olivine + antigorite + Mg-chlorite) is related to the high pressure (eclogite-facies) metamorphic peak. All the others vein generations developed during the retrograde evolution, at different *P-T* conditions, moderate for types 3 (carlosturanite + antigorite + diopside + garnet) and 4 (antigorite + diopside) and low or very low for types 5 (chrysotile), 6 (tremolite + calcite) and 7 (brucite + magnetite and talc + calcite).

Detailed petrographic analysis of the metamorphic veins occurring in the serpentinites gives information complementary to the conventional thermobarometric estimates based on the associated basic rocks and consequently is a powerful method to reconstruct the *P-T* path of the ophiolitic units.

* Corresponding author, E-mail: chiara.groppo@unito.it

RIASSUNTO. — Lo studio petrografico in sezione sottile ed in spettroscopia micro-Raman delle vene metamorfiche presenti nelle serpentiniti della Zona Piemontese (Alpi Occidentali) ha permesso di riconoscerne sette differenti generazioni, sviluppatesi a diverse condizioni *P-T-X*. La prima generazione (balangeroite + magnetite + leghe FeNi) si è formata durante l'evoluzione prograda delle serpentiniti, mentre la seconda (diopside + Ti-clinohumite + olivina + antigorite + Mg-clorite) è associata al picco metamorfico alpino in facies eclogitica. Tutte le altre generazioni di vene si sono sviluppate durante l'evoluzione retrograda, a differenti condizioni *P-T*, moderate per le vene di tipo 3 (carlosturanite + antigorite + diopside + granato) e 4 (antigorite + diopside) e basse o molto basse per le vene di tipo 5 (crisotilo), 6 (tremolite + calcite) e 7 (brucite + magnetite e talco + calcite).

Lo studio petrografico di dettaglio delle vene metamorfiche presenti nelle serpentiniti fornisce informazioni complementari alle stime termobarometriche convenzionali ricavabili dalle rocce basiche associate, ed è quindi un metodo molto valido per ricostruire le traiettorie *P-T* delle unità ofiolitiche.

KEY-WORDS: *Piemonte Zone, serpentinites, metamorphic veins, micro-Raman spectroscopy*

INTRODUCTION

The reconstruction of the *P-T* path for a tectonometamorphic unit consisting of ultramafics is generally difficult for the following reasons:

− most reactions in the ultramafic system are temperature dependent and give no information about pressure (see e.g. Evans *et al*., 1976; Evans, 2004);

− stability fields of serpentine minerals span a large *T*-interval and are poorly constrained towards low temperatures. Moreover, thermodynamic properties of minerals in the MSH system are highly uncertain and there are many lines of evidence that chrysotile has not a true stability field but that its development is mainly controlled by nucleation and growth conditions (Evans, 2004);

− serpentine minerals easily recrystallize, thus obliterating microstructural relationships acquired during prograde metamorphism.

In the Piemonte Zone of Calcschists with meta-ophiolites (western Alps), the relict peridotites have been studied by Nicolas (1966), Boudier (1971, 1976), Compagnoni *et al.* (1980), Bodinier, (1988), Rossetti and Zucchetti (1988a,b) and Piccardo *et al.* (2004a,b), whereas little attention was given to serpentinite until the International Conference on Asbestos held in Turin (Italy) in 1980 (Compagnoni *et al.*, 1980). New minerals were discovered in several serpentinite bodies from the Piemonte Zone, namely balangeroite and carlosturanite (Compagnoni *et al.*, 1983, 1985; Mellini *et al.*, 1985; Mellini, 1986; Ferraris *et al.*, 1987; Belluso and Ferraris, 1991), and different metamorphic vein types were recognised (Compagnoni *et al.*, 1980; Alberico *et al.*, 1997). However, a petrological study of serpentinites of the Piemonte Zone and related metamorphic veins is still lacking.

The purpose of this paper is to describe petrologically the different generations of metamorphic veins occurring in the serpentinites from the Piemonte Zone, each of them being characterized by a distinctive paragenesis. Microstructural relationships among these veins have allowed interpretation of their relative chronology and the study of their mineralogy has permitted constraints to be applied to their genetic *P-T* conditions. It is concluded that the detailed petrographic analysis of metamorphic veins occurring in serpentinites is a powerful method for reconstructing the *P-T* path of ophiolitic units, and for giving complementary information with respect to the conventional thermobarometric estimates based on the associated metabasics.

GEOLOGICAL SETTING

Most serpentinites of the western Alps crop out in the Piemonte Zone of Calcschists with meta-ophiolites, a remnant of the Piemontese Ocean that opened in the Late Jurassic between the European continent to the NW and the Apulia Plate to the SE (see e.g. Dewey *et al.*, 1989; Polino *et al.*, 1990). The Piemonte Zone (Fig. 1) mainly consists of calcschists with intercalations of different ophiolitic bodies. It is bounded by the blueschist-facies Briançonnais Zone to the west and by the eclogite facies Internal Crystalline Massifs to the east, both derived from the thinned European paleomargin. The studied serpentinite samples were collected from three different portions of the Piemonte Zone: the Lanzo Ultramafic Massif, the Internal Piemonte Zone and the External Piemonte Zone (Fig. 1).

The Lanzo Ultramafic Massif is located in the innermost part of the Piemonte Zone. It is a large body of fresh tectonitic spinel-plagioclase lherzolite with subordinate harzburgite and rare dunite, partially converted to antigorite-serpentinite at the rim and along shear zones (Nicolas, 1966; Boudier, 1976; Compagnoni *et al.*, 1980; Pognante *et al.*, 1985; Bodinier, 1988). According to many authors (Pognante *et al.*, 1985; Rampone and Piccardo, 2000; Müntener *et al.*, 2004; Piccardo *et al.*, 2004a,b), the Lanzo Massif is a portion of sub-continental lithosphere emplaced at shallow levels during the opening of the Mesozoic Piemontese-Ligurian basin and subsequently involved in the subduction processes associated with the closure of the ocean. The polyphase Alpine metamorphic evolution, well recorded in the serpentinized portion of the Lanzo Massif, consists of a first oceanic stage followed by an orogenic high pressure, eclogite-facies, peak (Compagnoni *et al.*, 1980; Bodinier, 1988; Pognante, 1991). Petrologic studies of the basic rocks associated with serpentinites indicate peak conditions of 500-550°C and 15-16 kbar (Compagnoni *et al.*, 1980; Pognante, 1991) or

550-620°C and pressures in excess of 20 kbar (Pellettier and Müntener, 2006). During the post-climax exhumation, the Lanzo Massif experienced a clockwise *P-T* path from eclogite- to greenschist-facies conditions (Compagnoni *et al.*, 1980; Pognante, 1991; Castelli *et al.*, 1995).

In both the Internal and External Piemonte Zone, serpentinite, metagabbro and metabasalt occur at the base of the stratigraphic sequence; they are covered by calcschists and siliceous marbles, which include detrital horizons and olistostromes with blocks of serpentinites and metagabbros (Lemoine and Tricart, 1986). In the Internal Piemonte Zone, both the basement and the associated sediments are characterized by peak eclogite-facies parageneses. The peak metamorphic conditions range from 500-550°C and 15-16 kbar in the south to 550-600°C and 25-30 kbar in the north (Barnicoat and Fry, 1986, 1989; Reinecke, 1991, 1995; Cartwright and Barnicoat, 2002; Li *et al.*, 2004; Bucher *et al.*, 2005). During the late exhumation history, the Internal Piemonte Zone followed a decompressional path associated with a significant temperature decrease.

The External Piemonte Zone is characterized by peak lawsonite to epidote-blueschist facies parageneses. The peak metamorphic conditions range from 350-400°C and 14-15 kbar (in the lawsonite stability field; Oberhänsli *et al.*, 1995; Agard *et al.*, 2001) to 400-500°C and *P*=14-15 kbar (in the epidote stability field). The exhumation *P-T* path was characterized by a decompression associated with a significant cooling (Agard *et al.*, 2000).

Sample localities with indications of the different vein types recognized in the serpentinites have been reported in Fig.1.

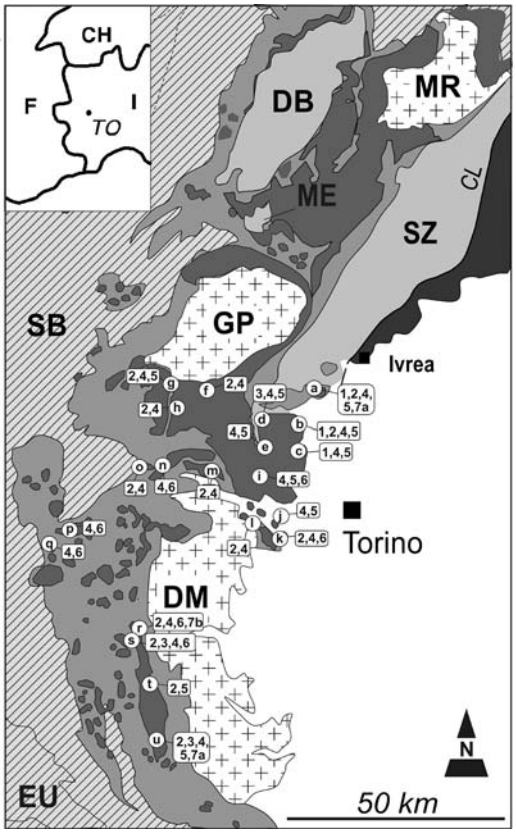

Fig. 1 – Simplified tectonic sketch-map of the inner part of the Italian western Alps. Penninic Domain: Grand St. Bernard Zone (SB), Monte Rosa (MR), Gran Paradiso (GP) and Dora-Maira (DM) Internal Crystalline Massifs, and Piemonte Zone of Calcschists (light grey) with meta-Ophiolites (dark grey); Austroalpine Domain: Dent Blanche nappe (DB), Monte Emilius nappe (ME), and Sesia Zone (SZ); Southern Alps (black); Embrunais-Ubaye Flysch nappe (EU); Canavese line (CL).
Sample locations and vein types (from type 1 to 7) are indicated. Lanzo Valleys: a) Balangero, b) Lanzo, c) Varisella, d) Fubina, e) M. Crusat, f) Chiampernotto, g) Balme, h) P.ta della Rossa; Susa Valley: i) Col del Lys, j) Moncuni, k) Trana, l) S.Ambrogio, m) Mollette, n) Mompantero, o) Seghino, p) Oulx, q) Argentiera; Pellice Valley: r) Villanova, s) Col Barant; Po Valley: t) Lago Chiaretto; Varaita Valley: u) Sampeyre OF3255.

Analytical methods

Despite the relatively simple chemical composition of the ultramafic system, serpentinites are often difficult to interpret petrologically because they are characterized by a wide variety of microstructures (Wicks and Whittaker, 1975, 1977; Wicks *et al.*, 1977; Wicks and Plant, 1979, Wicks and O'Hanley, 1988) and the serpentine minerals have very similar optical properties, are often very fine-grained and are frequently sub-microscopically intergrown, especially in veins where they exhibit a fibrous habit. As a consequence, the petrological study of serpentinites and their metamorphic veins requires a detailed characterization of the major minerals using different and complementary

analytical techniques, such as optical microscopy (both transmitted and reflected light), scanning electron microscopy with microanalysis (SEM-EDS), electron microprobe analyzer (EMPA-WDS), transmission electron microscopy (TEM), and micro-Raman spectroscopy (μ-Raman).

More than two hundred thin sections have been observed under the polarized light microscope, both in transmitted and reflected light. Among them, about fifty samples were analysed with a Cambridge Stereoscan 360 SEM equipped with an EDS Energy 200 (Oxford Instruments) at Dept. of Mineralogical and Petrological Sciences, the University of Torino, Italy. The operating conditions were: 50 s counting time and 15 kV accelerating voltage.

Check analyses on serpentine minerals, balangeroite and carlosturanite were also carried out with an electron microprobe (EMPA) Jeol JXA-8600 equipped with wavelength dispersive spectrometers (WDS) at C.N.R. – Institute of Geosciences and Georesources, Section of Florence (Italy). The operating conditions were 15 kV accelerating voltage and 10 nA beam current. The raw data were calibrated on natural mineral standards and corrected using the B-A method (Bence and Albee, 1968). Si, Fe, Al, Mg and Ti counts were collected for 15 s and Mn, Ca, Cr and Ni counts for 40 s, respectively. SEM-EDS and EPMA-WDS analyses on fibrous vein minerals have been obtained on bundles of fibres rather than on a single fibre, the fibre diameter being lower than 1 μm. However, the close similarity of the spot analyses allows us to consider our analyses as quantitative.

Chemical analyses of serpentine were normalised on the basis of 7 anhydrous oxygens, and Al has been allocated into both octahedral and tetrahedral sites to obtain the full occupancy of the tetrahedral site. The antigorite chemical formula reported by Kunze (1961), based on the number of tetrahedra along an entire wavelength (*m*), is $Mg_{3m-3}Si_{2m}O_{5m}(OH)_{4m-6}$. Thus, when m = 17, antigorite (that from veins of type 4) has 116 "anhydrous" oxygens and a normalization for 2 silicons would be referred to 6.824 oxygens. However, the *m* parameter of antigorite was not determined for all the samples and for this reason all the antigorites were normalized to 7 oxygens. This may result in a slight underestimation of the Al^{IV} content.

Balangeroite and carlosturanite chemical analyses were normalised to 16 and 12 (Si+Al), respectively (Mellini *et al.*, 1985; Mellini and Zussman, 1986; Belluso and Ferraris, 1991), and all Fe has been considered as Fe^{+2}. Tremolite was normalized to 23 oxygens and 15 cations.

Micro-Raman spectroscopy has been used as a technique complementary to optical microscopy and SEM-EDS for rapid serpentine mineral identification (Rinaudo *et al.*, 2003; Groppo *et al.*, 2006). Micro-Raman spectra were acquired using an integrated micro/macro Raman system Horiba Jobin Yvon HR 800 at the Dept. of Mineralogical and Petrological Sciences, the University of Torino (Italy) and at the Dipartimento di Scienze dell'Ambiente e della Vita, University of Piemonte Orientale, Alessandria (Italy). Both systems include a microspectrometer Horiba Jobin Yvon HR800, an Olympus BX41 microscope and a CCD air-cooled detector. A polarised solid state Nd 80 mW laser operating at 532.11 nm was used as the excitation source for the instrument in Torino, whereas a HeNe 20 mW laser working at 632.8 nm was used in Alessandria. Correct calibration of the instruments was verified by measuring the Stokes and anti-Stokes bands and checking the position of the Si band at ± 520.7 cm^{-1}. Each spectrum was acquired using a 50X objective, resulting in a laser beam size at the sample on the order of 10 μm. To optimize the signal to noise ratio, spectra were acquired using 10 scans of 10 seconds for each spectral region.

A few samples of fibrous antigorite and chrysotile were also observed by Transmission Electron Microscopy (TEM) using Selected Area Electron Diffraction (SAED), in order to recognise the possible existence of sub-microscopic intergrowths not visible with the SEM. TEM observations were carried out at the Dept. of Mineralogical and Petrological Sciences, the University of Torino, Italy, using a Philips CM12 instrument operating at 120 kV. The samples were prepared by suspending the powder in isopropylic alcohol; fibre aggregation was minimized by means of ultrasound treatment, and several drops of the suspension were deposited on carbon supported Cu grid.

Petrography

Serpentinite microstructures

In the Lanzo Massif and in the Piemonte Zone, the ultramafic rocks show different degrees of serpentinization of the peridotitic protolith and are characterized by different microstructures: they can either preserve relics of the peridotitic paragenesis or be completely serpentinized. Serpentinites lacking deformation and therefore less recrystallized generally show a *mesh* or *hourglass* structure (Wicks *et al.*, 1977; Wicks and Whittaker, 1977; Wicks and Plant, 1979) mainly consisting of lizardite (Figs. 2a,b). Orthopyroxene is replaced by "bastite" pseudomorphs consisting of lizardite, antigorite (Figs. 2c,d) or fine-grained diopside aggregates. Peridotitic clinopyroxene is generally preserved, or partially replaced by metamorphic diopside, olivine + Ti-clinohumite or oriented antigorite + tremolite aggregates. Peridotitic spinel is replaced by Cr-magnetite at the core and Mg-chlorite at the rim (Compagnoni *et al.*, 1980). The most recrystallized serpentinites generally show an *interpenetrating* or *interlocking* microstructure consisting of antigorite ± magnetite (Wicks and Whittaker, 1977) (Figs. 2e,f). Opaque minerals are quite abundant and consist of native metals (Fe-Ni alloys and rare iron), oxides (magnetite) and sulphides (pentlandite, heazlewoodite and pyrrhotite). Fe-Ni alloys are generally limited to partially serpentinized peridotites, their formation being controlled by the degree of serpentinization (Ramdohr, 1967; Eckstrand, 1975; Frost, 1985; Rossetti *et al.*, 1987; Rossetti and Zucchetti, 1988a,b).

Most analyzed serpentinites are crosscut by metamorphic veins, which give information about the metamorphic *P-T* conditions, the nature of the metamorphic fluids, and their genetic deformation mechanisms. Seven different generations of metamorphic veins have been recognized, most of them including fibrous minerals. Microstructural relationships between the different vein generations and the hosting serpentinites are described in the following.

Metamorphic veins

Type 1 veins – Balangeroite + magnetite + Fe-Ni alloys (+ chrysotile)

The earliest generation of metamorphic veins consists of fibrous balangeroite (Fig. 3a) + magnetite + Fe-Ni alloys and is limited to the serpentinized rim of the northern Lanzo Ultramafic Massif (Compagnoni *et al.*, 1983; Belluso and Ferraris, 1991); they are particularly abundant in the Balangero asbestos mine, where balangeroite was firstly discovered (Compagnoni *et al.*, 1983). These veins show slip fibres often deformed and folded (Fig. 3b).

Balangeroite occurs as brown rigid fibres, up to 10 cm long (Fig. 3a) (Groppo *et al.*, 2005), with a distinct pleochroism: dark brown and yellow brown parallel and perpendicular to the fibre elongation [001], respectively. Careful examination of several thin sections has allowed us to observe that fibrous balangeroite may develop at the expense of prismatic balangeroite, only locally preserved (Fig. 3c). Relict prismatic balangeroite often includes antigorite flakes. TEM observations (Ferraris *et al.*, 1987) clearly show that fibrous balangeroite is partially replaced by chrysotile, which starts to develop at the junction among balangeroite fibres.

In this vein generation magnetite is the most abundant opaque phase, but Fe-Ni alloys (awaruite and taenite) and pentlandite are also present. Fibrous balangeroite is statically overgrown by metamorphic olivine and diopside (Fig. 3d), both belonging to the peak-*P* eclogite-facies assemblage.

Type 2 veins – Diopside + Ti-clinohumite + olivine + Mg-chlorite + antigorite + magnetite

The second vein generation consists of diopside + Ti-clinohumite + olivine + Mg-chlorite + antigorite + magnetite and is widespread all over the Internal Piemonte Zone. These veins, from few millimetres to several centimetres thick (Fig. 3e), are often deformed and folded. Ti-clinohumite is always present and locally occurs as coarse-grained reddish-brown porphyroblasts visible in the hand sample. Ti-clinohumite shows a marked pleochroism, from yellow to dark orange, and is often associated to porphyroblastic metamorphic olivine (Fig. 3f) and, less frequently,

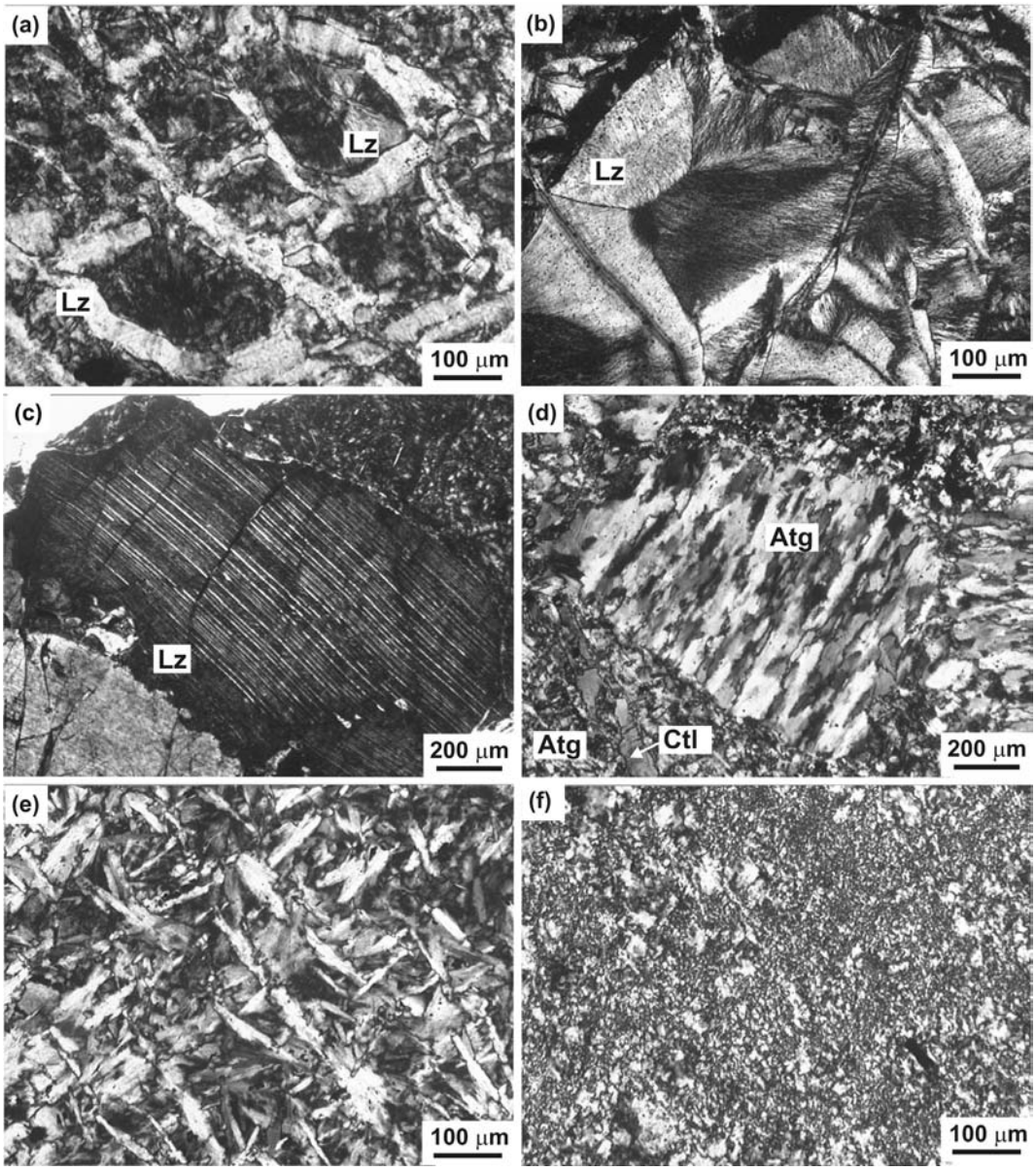

Fig. 2 – Representative microstructures of serpentinites from the Piemonte Zone, western Alps, as seen under optical microscope. (a) Lizardite with mesh structure after peridotitic olivine: the mesh rim consists of apparent fibres oriented perpendicularly to the mesh boundaries; the mesh core mainly consists of fine grained random lizardite. OF2830, Crossed Polarized Light (XPL). (b) Lizardite with hourglass microstructure. OF1427, XPL. (c) "Bastite" after peridotitic orthopyroxene consisting of lizardite (Lz). The original clinopyroxene exsolutions are still visible, although totally replaced by lizardite with different optical orientation. OF2889, XPL. (d) Oriented antigorite (Atg) flakes replacing a peridotitic clinopyroxene. OF2874, XPL. (e) Serpentinite matrix (antigorite) with interpenetrating microstructure. OF1816, XPL. (f) Serpentinite matrix with interlocking microstructure. OF2827, XPL.

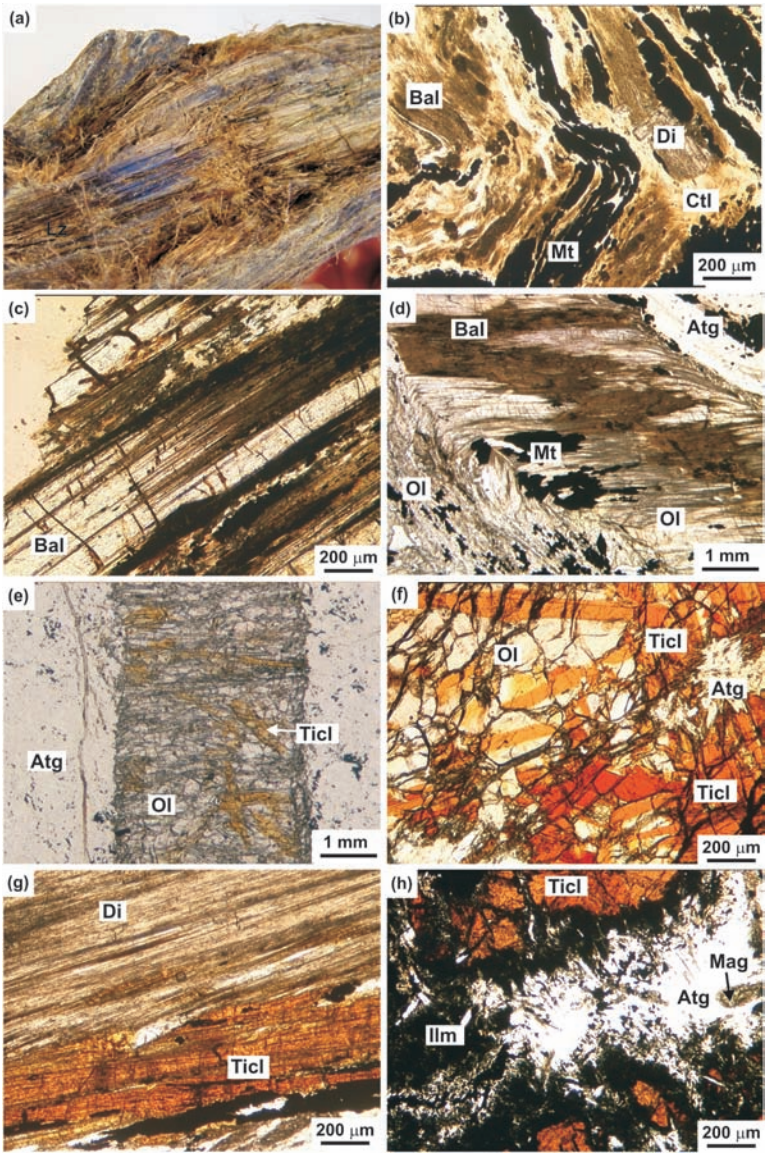

Fig. 3 – Representative microstructures of veins of type 1 and 2. *Type 1 veins*: (a) Fibrous balangeroite as seen in hand sample. The fibres are about 10 cm long. (b) Veins of type 1 consisting of deformed and folded balangeroite (Bal), chrysotile (Ctl) and magnetite (Mt). Idioblastic diopside (Di) statically overgrows the fold hinge. OF2838, Plane Polarized Light (PPL). (c) Prismatic balangeroite (Bal) partially replaced by its fibrous variety. OF1645, PPL. (d) Peak metamorphic olivine (Ol) which had statically overgrown folded fibrous balangeroite (Bal). OF3183, PPL. *Type 2 veins*: (e) Vein of type 2 consisting of granoblastic olivine (Ol), Ti-clinohumite (Ticl) and minor fibrous diopside. OF2957, PPL. (f) Olivine (Ol), Ti-clinohumite (Ticl) and antigorite (Atg) from vein of type 2. OF3186, PPL. (g) Fibrous diopside (Di) and Ti-clinohumite (Ticl). OF2954, PPL. (h) Ti-clinohumite (Ticl) partially replaced at its margins by a radiating intergrowth of ilmenite (Ilm) + antigorite (Atg) + magnesite (Mag). OF3270, PPL. (f) Olivine, Ti-clinohumite and antigorite from vein of type 2. OF3186, PPL. (g) Fibrous diopside and Ti-clinohumite. OF2954, PPL. (h) Ti-clinohumite partially replaced at its margins by a radiating intergrowth of ilmenite + antigorite + magnesite. OF3270, PPL.

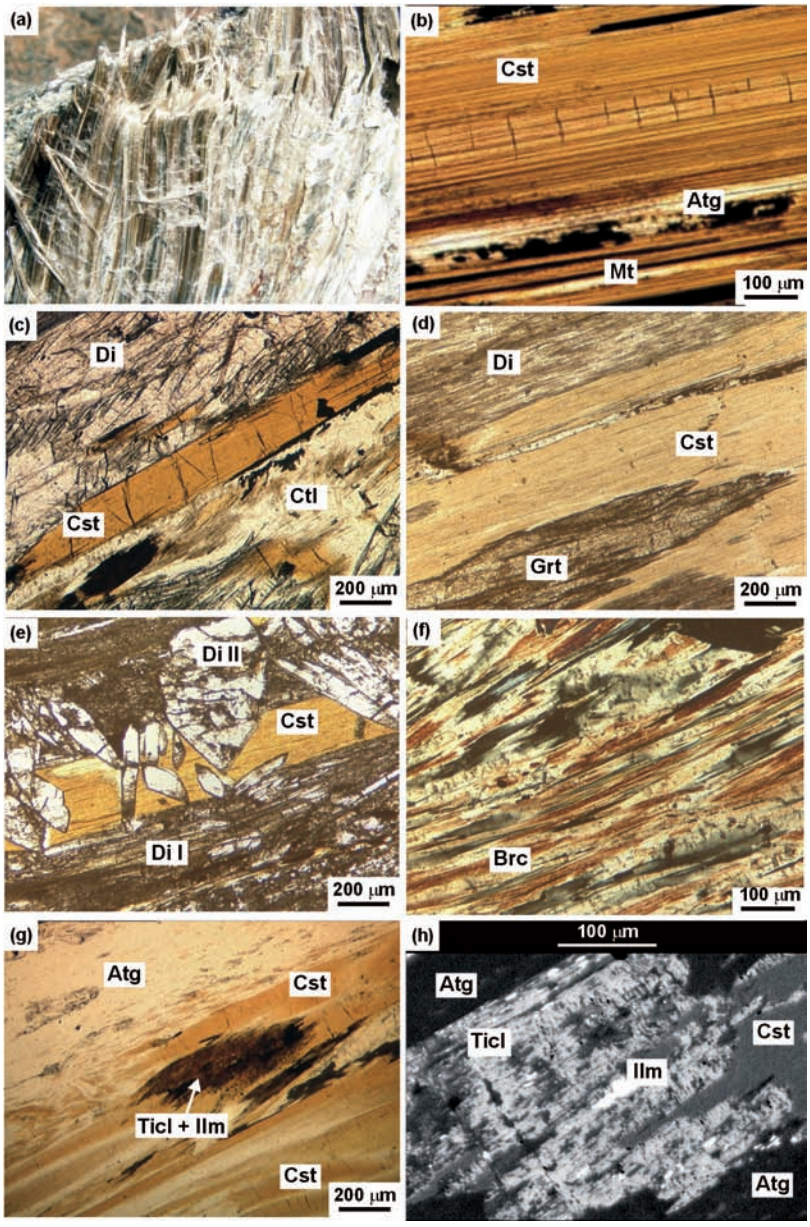

Fig. 4 – Representative microstructures of veins of type 3. (a) Carlosturanite associated with long fiber chrysotile, as seen on hand specimen. The fibers are about 10 cm long. (b) Carlosturanite as seen under the optical microscope (PPL). Fractures perpendicular to the fibre elongation are evident. (c) Prismatic carlosturanite (Cst) partially replaced by fibrous carlosturanite at the ends. OF3255, PPL. d) Fibrous diopside (Di) and garnet (Grt) associated with carlosturanite in type 3 vein. OF3077, PPL. (e) Idioblastic diopside (Di II) statically overgrowing carlosturanite (Cst) and diopside (Di I) of vein of type 3. OF3089, PPL. (f) Fibrous brucite replacing carlosturanite in vein of type 3. OF3082, XPL. (g) Carlosturanite replacing a dusty aggregate composed of Ti-clinohumite + ilmenite. OF3255, PPL. (h) Back Scattered Electron image showing carlosturanite replacing former Ti-clinohumite.

to paler coloured humite. Ti-clinohumite is locally replaced at the margins by a radiating intergrowth of elongate ilmenite + antigorite + magnesite (Fig. 3h).

Diopside is always present in this vein generation. It generally occurs as small idioblasts with preferred orientation and concentrated in monomineralic domains, which alternate with Ti-clinohumite + olivine + Mg-chlorite domains. In most analysed samples, diopside and, though less frequently, also Ti-clinohumite, may develop a fibrous habit (Fig. 3g). Fibrous diopside occurs as whitish bundles, up to several centimetres long, brittle and rigid, locally replaced by tremolite. Mg-chlorite and antigorite are the supplementary minerals of the type 2 veins. Mg-chlorite, which shows brownish anomalous interference colours, occurs as large flakes in the Ti-clinohumite-rich domains, whereas antigorite occurs as random idioblastic flakes locally partially replacing Mg-chlorite.

Type 3 veins – Carlosturanite + antigorite + diopside + garnet (+ chrysotile + brucite)

The third vein generation, from a few millimetres to several centimetres thick, consists of carlosturanite + antigorite + diopside + garnet and is widespread in the serpentinites of the Internal Piemonte Zone, from the Viù Valley to the north to the Maira Valley to the south (Belluso and Ferraris, 1991). They are particularly abundant in the serpentinites from the Auriol asbestos mine (Sampeyre, Val Varaita), where carlosturanite was first discovered (Compagnoni *et al.*, 1985).

Carlosturanite and diopside are the main constituents. Carlosturanite generally occurs as long fibres (Fig. 4a) oriented either parallel or perpendicular to the vein selvages, but it has been less frequently observed as elongated prismatic crystals, both varieties showing peculiar (001) cleavage (Figs. 4b,c). It shows a marked pleochroism, with orange-brownish and pale orange-brownish parallel and perpendicular to [010], respectively. Fibrous diopside, garnet and antigorite are intergrown with carlosturanite, as already reported by Compagnoni *et al.* (1985) (Figs. 4b,d). Diopside generally occurs in two different generations: a first fibrous diopside generation (Di I) as long fibres closely intergrown and clearly in equilibrium with carlosturanite, and a second diopside generation (Di II) as prismatic idioblasts statically overgrowing both fibrous carlosturanite and Di I (Fig. 4e). The more rare fibrous antigorite appears in equilibrium with carlosturanite (see also Belluso and Ferraris, 1991): it is preserved only in the less retrogressed samples. An andraditic garnet with fibrous habit is also frequently intergrown with carlosturanite and diopside (Fig. 4d).

Locally, carlosturanite appears to replace a dusty phase under optical microscope (Fig. 4g), which was identified by means of SEM-EDS and micro-Raman spectroscopy as a relict Ti-clinohumite replaced by carlosturanite + serpentine + ilmenite ± perovskite (Fig. 4h). Carlosturanite is often partially replaced by chrysotile and/or brucite, especially in the samples from the Varaita Valley. TEM images (Mellini *et al.*, 1985; Baronnet and Belluso, 2002) show that chrysotile and brucite are frequently associated. Brucite often exhibits a fibrous habit as the result of a pseudomorphic replacement of a single carlosturanite fibre (Fig. 4f).

Type 4 veins – Antigorite ± diopside

The fourth vein type, consisting of fibrous antigorite ± diopside is the most widespread vein type in the serpentinites from both the Internal and External Piemonte Zone (Groppo and Compagnoni, 2007). These veins, typically 1 to 20 cm thick and a few centimetres to several decimetres long, consist of rigid and brittle bundles of fibres with massive appearance in the hand specimen (Fig. 5a), light greyish-whitish to pale green in colour and with a splintery fracture. The contact with the host rocks is sharp and the fibres, up to 15-20 cm in length, are generally oriented perpendicularly to the vein selvages (Figs. 5b-d). In thin section, the fibrous antigorite-bearing veins show a peculiar banded structure parallel to the vein selvages, very similar to that described by Riordon (1955), Viti (1995), and Viti and Mellini (1996) (Figs. 5c,d). Small random diopside idioblasts locally occur in the centre of the vein (Fig. 5b). Elongated magnetite crystals may be present between adjacent fibres or at the vein selvages. These veins are often crosscut by slip and/or cross fibre chrysotile veins.

Two representative antigorite samples were observed by TEM using SAED. The average

supercell periodicities of the two studied specimens, measured on different SAED patterns, were 43.8 and 43.0 Å, respectively, which correspond to *m* values of 17 on the base of the data from Mellini *et al*. (1987). This *m* value is the most frequent value reported by Mellini *et al.* (1987), Wunder *et al.* (2001), Bromiley and Powley (2003) and Evans (2004) for antigorite formed under greenschist facies conditions.

Type 5 veins – Chrysotile

The fifth vein generation consists of chrysotile ± magnetite. These veins, a few millimetre thick, are particularly abundant in the northern portion of the Lanzo Massif, where they were exploited in the Balangero asbestos mine. Chrysotile fibres may be oriented either perpendicular or parallel to the vein selvages and in some cases show a banded microstructure (Fig. 5e-h), similar to that described by Andreani *et al.* (2004).

Type 6 veins – Tremolite ± calcite

The last vein generation consists of tremolite ± calcite and occurs both in the small serpentinite lenses embedded within the calcschists of the External Piemonte Zone and in the eclogite-facies serpentinites from the Internal Piemonte Zone. Tremolite occurs as white soft fibres (Fig. 6a), up to few centimetres long and generally oriented perpendicular to the vein selvages (Fig. 6b), often associated with calcite. The vein - host rock contact is sharp.

Other vein types: brucite + magnetite (type 7a) and talc + calcite (type 7b)

Occasionally, two other vein types have been observed, both relatively late in the serpentinite evolution. Brucite + magnetite veins (Fig. 6c) have been observed both in the Balangero asbestos mine and in the Monviso serpentinites. Brucite occurs as oriented flakes always associated with idoblastic magnetite. The talc + calcite veins (Fig. 6d) have been rarely recognised in the Monviso serpentinites. They are several millimetres thick and both talc and calcite occur with a fibrous habit, fibres being oriented perpendicularly to the vein selvages.

MINERAL CHEMISTRY

Chrysotile and antigorite

Chrysotile and antigorite from types 1, 2, 3, 4 and 5 veins are generally characterized by different (only partially overlapped) compositional fields, which can be clearly shown in a Al *vs.* Si/(Σ octahedral cations) diagram (Fig. 7).

SEM-EDS and WDS analyses show that the long fibre chrysotile replacing balangeroite and carlosturanite in type 1 and 3 veins, respectively, is characterized by high Al_2O_3 content (up to 4-5 wt%), rarely reported in the geologic literature (Albino, 1995) (Fig. 7a and Table 2). Normalizing the microprobe analyses to 7 anhydrous oxygens, about half of this Al is allocated into the tetrahedral site (up to 0.18 a.p.f.u.). In contrast, chrysotile from type 5 veins shows a variable chemical composition (Fig. 7c), which probably reflects the local bulk rock composition: its Al_2O_3 and FeO contents range from less than 1.0 wt% up to 4.5-5.5 wt% and from less than 1.0 wt% up to 4.0-5.0 wt%, respectively. Also the Ni content may be relatively high (up to 1.5 wt%) (Table 2).

Antigorite flakes occurring in type 2 veins has a relatively high Al and Fe contents (up to 0.14 and 0.13 a.p.f.u., respectively, on the basis of 7 anhydrous oxygens) (Fig. 7b and Table 4), whereas antigorite associated with carlosturanite in type 3 veins is chemically homogeneous and contains very little Al (Fig. 7b), all allocated into the octahedral sites (normalization on the basis of 7 anhydrous oxygens) (Table 4).

Chemical SEM-EDS and EMPA-WDS analyses from different samples of fibrous antigorite in type 4 veins are quite homogeneous and consistent with literature data (Wicks and Whittaker, 1975, 1977; Wicks and Plant, 1979; Dungan, 1979; Mellini *et al.*, 1987; Viti, 1995; Viti and Mellini, 1996). Its Al content in the tetrahedral sites is very low (Al^{IV} = 0.00-0.08 a.p.f.u.) and Mg in the octahedral sites is partly replaced by Al (0.04-0.15 a.p.f.u.) and Fe (0.07-0.22 a.p.f.u.) (Fig. 7d and Table 4). Cr is rarely present, whereas Ni has been detected in few samples only by means of WDS, being below the EDS detection limit (NiO = 0.14-0.15 wt%). This fibrous antigorite from type 4 veins is characterized by lower Fe and Al contents with respect to antigorite from type 2 veins.

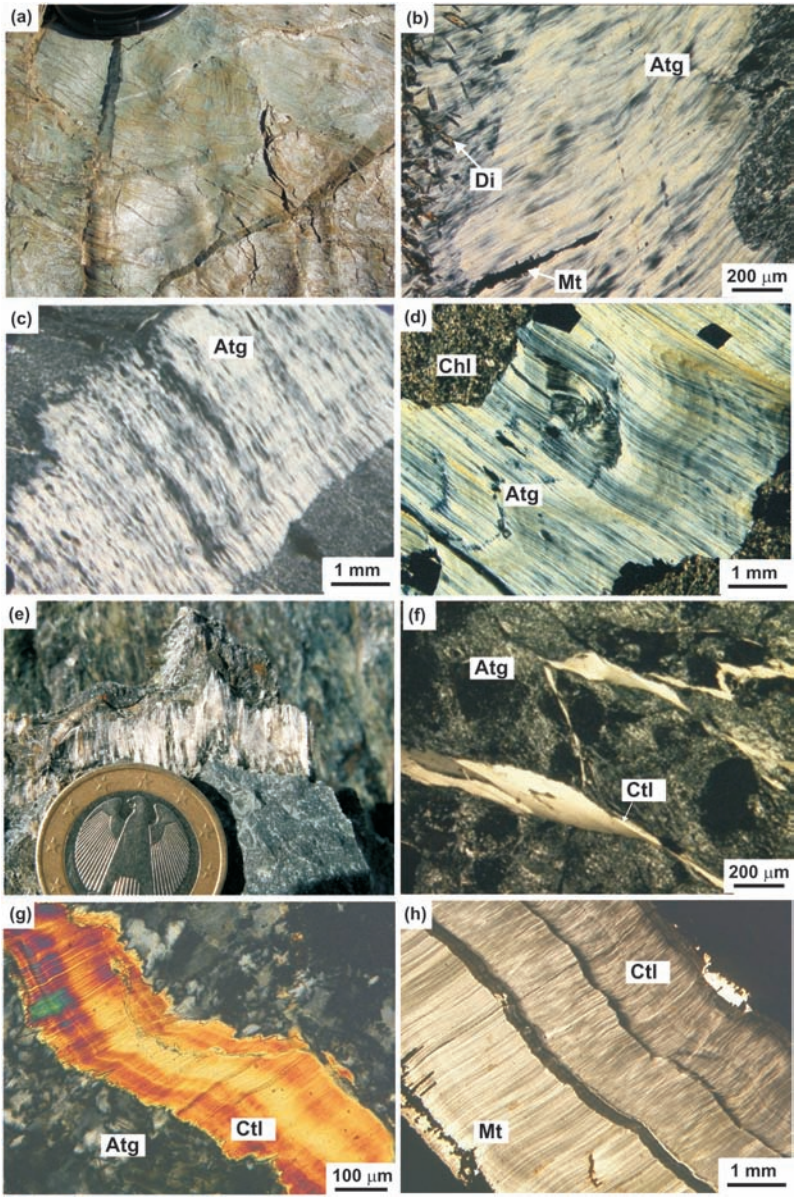

Fig. 5 – Representative microstructures of veins of type 4 and 5. *Type 4 veins*: (a) Fibrous antigorite veins as seen on the outcrop. The camera cap is 6 cm wide. (b) Type 4 vein consisting of fibrous antigorite (Atg) and idioblastic diopside (Di) in the centre of the vein. Magnetite (Mt) locally occurs as needle-like crystals grown parallel to the antigorite fibers. OF2831, XPL. (c) Fibrous antigorite vein with a banded structure parallel to the vein selvages. OF2956, XPL. (d) Fibrous antigorite vein with a banded structure which is parallel to the vein selvages. OF3204, XPL. *Type 5 veins*: (e) Chrysotile veins as seen on the outcrop. (f) Slip chrysotile vein of type 5 crosscutting an antigorite (Atg) serpentinite with interlocking structure. OF2827, XPL. (g) Cross fiber chrysotile vein with a banded structure parallel to the vein selvages. OF2874, XPL. (h) Cross fiber chrysotile (Ctl) in a crack-seal vein of type 5. The vein is characterized by a banded structure parallel to the vein selvages. Magnetite (Mt) is concentrated at the vein selvages or is grown parallel to chrysotile fibres. OF2892, XPL.

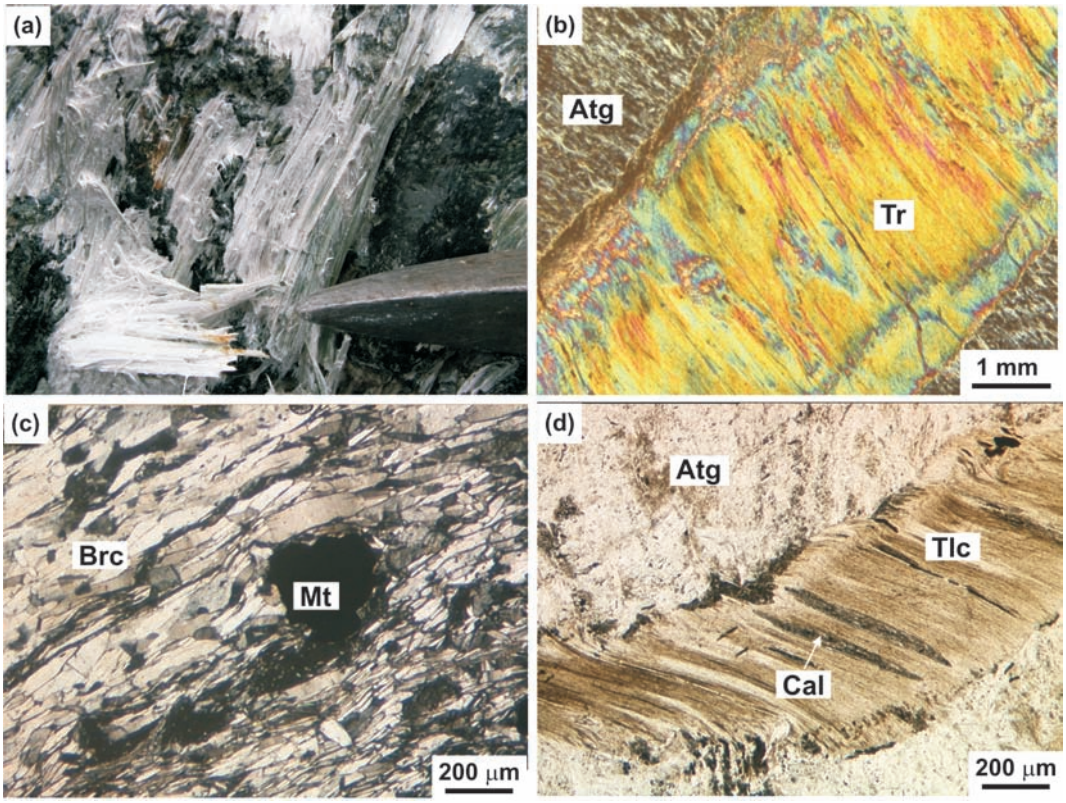

Fig. 6 – Representative microstructures of veins of types 6 and 7. *Type 6 veins*: (a) Fibrous tremolite (Tr) veins as seen on the outcrop. (b) Cross fibre tremolite vein crosscutting a foliated antigorite (Atg) matrix. OF3200, XPL. *Type 7 veins*: (c) Type 7a brucite (Brc) + magnetite vein. OF2946, XPL. (d) Type 7b talc (Tlc) + calcite (Cal) vein in an antigorite matrix (Atg). OF3265, PPL.

Balangeroite and carlosturanite

The chemical composition of fibrous balangeroite from type 1 veins is quite homogeneous, whereas relict prismatic balangeroite shows a wider compositional range, suggesting a solid solution series between a Mg-rich and a Fe-rich end-member (Fig. 8a and Table 1). Chemical analyses, normalized to 16 (Si+Al), give a Σ(M cations) of about 42, in agreement with the structural formula proposed by Compagnoni *et al.* (1983). A Fe^{+3} content of about 20% of Fe_{tot} has been determined using Mössbauer spectroscopy (Deriu *et al.*, 1994).

Carlosturanite occurring in type 3 veins from the Viù Valley shows the highest Ti content, whereas carlosturanite from the Pellice Valley has the highest Mg content (Fig. 8b). Chemical analyses, normalized to 12 (Si+Al), give Σ(M cations) in the range 21.1–23.3 and the highest Σ(M cations) values have been observed in the prismatic variety (Table 1). These Σ(M cations) values are higher than those proposed by Compagnoni *et al.* (1983) and Belluso and Ferraris (1991) (structural formula: $M_{21}[T_{12}O_{28}(OH)_4](OH)_{30}\cdot H_2O$) and are more similar to those reported by Kolitsch *et al.* (2003), which proposed the structural formula $M_{24}T_{12}O_{32}(OH)_{32}$ (M=Mg,Fe,Ti,Mn; T=Si,Al). A Fe^{+3} content of about 38% of Fe_{tot} has been determined using Mössbauer spectroscopy (Deriu *et al.*, 1994).

TABLE 1
Representative SEM-EDS analyses of balangeroite and carlosturanite

Vein type	**Type 1 - Balangeroite**						**Type 3 - Carlosturanite**					
	Fibrous			Prismatic			Fibrous			Prismatic		
Sample	OF2837	OF2838	OF2950	OF2855	OF2950	OF2951	OF3077	OF3082	OF2864	OF3255	OF3255	OF3255
Locality	(a)	(a)	(c)	(b)	(c)	(c)	(u)	(u)	(d)	(s)	(s)	(s)
Analyses	6.3	7.1	2.4	4.2	2.2	6.21	1.6	5.1	6.1	1.9	2.5	4.4
SiO_2	28.51	28.16	28.00	27.37	28.18	27.22	35.76	35.50	34.35	33.94	33.99	34.17
Al_2O_3	0.00	0.00	0.00	0.00	0.00	0.00	1.48	0.63	1.14	1.20	1.16	1.37
TiO_2	0.00	0.00	0.00	0.00	0.00	0.00	4.35	3.66	5.28	4.06	4.15	3.73
FeO	26.80	25.46	24.95	22.96	23.92	25.25	4.31	3.92	2.57	4.22	4.56	5.01
MnO	3.04	2.23	0.76	3.47	0.54	0.63	0.98	1.41	0.43	0.00	0.00	0.48
MgO	33.45	33.81	34.77	33.35	35.60	33.23	39.11	40.53	40.74	41.57	41.15	40.81
CaO	0.00	0.00	0.00	0.00	0.00	0.00	0.00	0.00	0.00	0.00	0.00	0.00
Total	91.81	89.66	88.48	87.15	88.24	86.33	85.99	85.65	84.51	84.99	85.01	85.57
Si	16.00	16.00	16.00	16.00	16.00	16.00	11.44	11.75	11.55	11.52	11.54	11.46
Al	0.00	0.00	0.00	0.00	0.00	0.00	0.56	0.25	0.45	0.48	0.46	0.54
Ti	0.00	0.00	0.00	0.00	0.00	0.00	1.05	0.91	1.34	1.04	1.06	0.94
Fe^{+2}	12.58	12.10	11.92	11.22	11.36	12.41	1.15	1.09	0.72	1.20	1.29	1.40
Mn	1.44	1.07	0.37	1.72	0.26	0.31	0.27	0.40	0.12	0.00	0.00	0.14
Mg	27.99	28.64	29.62	29.06	30.13	29.12	18.66	20.01	20.42	21.04	20.82	20.40
Ca	0.00	0.00	0.00	0.00	0.00	0.00	0.00	0.00	0.00	0.00	0.00	0.00
ΣM	42.01	41.81	41.91	42.01	41.75	41.84	21.12	22.40	22.60	23.27	23.17	22.88

TABLE 2
Representative SEM-EDS analyses of chrysotile

Vein type	Type 1		Type 3		Type 5					
Sample	OF2837	OF2838	OF3077	OF3213	OF2827	OF2863	OF2866	OF2889	OF2892	OF3271
Locality	(a)	(a)	(u)	(u)	(a)	(d)	(d)	(j)	(j)	(t)
Analyses	1.5	4.4	5.8	4.6	5.4	1.1	1.1	1.1	1.2	3.7
SiO_2	39.85	41.00	40.41	40.45	42.24	39.04	40.44	43.71	43.84	40.09
Cr_2O_3	0.00	0.00	0.00	0.00	0.00	0.50	0.44	0.00	0.00	0.00
Al_2O_3	5.35	2.60	4.17	3.50	2.93	4.47	4.67	0.83	0.77	3.73
FeO	3.33	4.69	3.37	3.15	2.50	4.92	3.05	1.87	2.27	2.85
MgO	38.54	38.98	37.55	38.99	39.35	37.01	38.64	40.65	40.32	39.49
NiO	0.00	0.00	0.00	0.00	0.00	0.98	0.00	0.00	0.00	0.00
Total	87.07	87.28	86.64	86.66	87.02	87.40	87.23	87.06	87.20	86.16
Si	1.87	1.93	1.91	1.91	1.98	1.86	1.90	2.05	2.05	1.90
Al^{IV}	0.13	0.07	0.09	0.09	0.02	0.14	0.10	0.00	0.00	0.10
Al^{VI}	0.17	0.08	0.14	0.10	0.15	0.11	0.16	0.05	0.04	0.10
Fe^{+3}	0.00	0.00	0.00	0.00	0.00	0.02	0.00	0.00	0.00	0.00
Fe^{+2}	0.13	0.18	0.13	0.12	0.10	0.20	0.12	0.07	0.09	0.11
Mg	2.70	2.74	2.64	2.74	2.76	2.62	2.71	2.84	2.81	2.78
Cr	0.00	0.00	0.00	0.00	0.00	0.02	0.02	0.00	0.00	0.00
Ni	0.00	0.00	0.02	0.00	0.00	0.04	0.00	0.00	0.00	0.00

Olivine, Ti-clinohumite and Mg-chlorite

Metamorphic olivine from type 2 veins shows a forsterite content ranging from Fo_{88} to Fo_{94}, depending on bulk chemical composition (Table 3). The Ti content of the Ti-clinohumite associated to this olivine is highly variable, from 0.14 to 0.81 a.p.f.u. (on the basis of 4 oxygens) (Table 3). Mg-chlorite from type 2 veins has a quite homogeneous chemical composition, plotting in the penninite field according to Hey (1954).

Diopside and tremolite

Diopside from types 2, 3 and 4 veins always shows a composition very close to the pure end-member (Table 3). Tremolite from type 6 veins has a composition close to the end member (i.e. $Ca/\Sigma M \approx 0.4$), with only little Fe (Fe^{+2} up to 0.40 a.p.f.u.) for Mg substitution (Fig. 8c and Table 3). The Fe-richer tremolite is generally greenish in colour and shows more rigid habit.

MICRO-RAMAN SPECTROSCOPY

Micro-Raman spectroscopy is useful for the rapid, reliable identification of serpentine minerals (lizardite, antigorite and chrysotile) (Rinaudo *et al.*, 2003; Groppo *et al.*, 2006), especially when they are fibrous and microscopically intergrown. For these reasons, this technique has been applied to the same thin sections previously examined by optical and electron microscopy. All the studied fibrous minerals from the different vein generations, i.e. balangeroite, carlosturanite, antigorite, chrysotile, tremolite, diopside, talc and brucite, are characterized by peculiar micro-Raman spectra (Table 5); only the most intense peaks are briefly described in the following. It is worthy to note that the intensity of the Raman peaks is strongly related to the sample orientation with respect to the laser incident beam, especially in the low-frequency region. A detailed spectral interpretation was reported by Rinaudo *et al.* (2003), Auzende *at*

TABLE 3
Representative SEM-EDS analyses of Ti-clinohumite, olivine, diopside and tremolite

	Ti-clinohumite		**Olivine**		**Diopside**					**Tremolite**			
Vein type	Type 2		Type 2		Type 2			Type 3		Type 6			
Sample	OF2900	OF2954	OF2900	OF2954	OF2900	OF2954	OF2957	OF3077	OF3077	OF3200	TrLz	TrOu	C1
Locality	(k)	(g)	(k)	(g)	(k)	(g)	(f)	(u)	(u)	(n)	(g)	(p)	(q)
Analyses	9.5	2.4	2.6	1.17	2.1	5.3	4.1	1.1	7.1	1.1	1.6	1.2	2.14
SiO_2	35.25	35.87	41.70	41.79	53.91	54.91	54.33	54.27	54.17	58.48	58.54	58.70	57.67
TiO_2	3.80	3.35	0.00	0.00	0.00	0.00	0.00	0.00	0.00	0.00	0.00	0.00	0.00
Cr_2O_3	0.00	0.00	0.00	0.00	0.00	0.00	0.00	0.00	0.00	0.00	0.00	0.00	0.00
Al_2O_3	0.00	0.00	0.00	0.00	0.00	0.00	0.00	0.00	0.00	0.47	0.00	0.00	0.73
FeO	15.66	6.17	4.82	5.76	1.85	0.00	1.19	0.86	0.79	1.94	2.71	1.55	1.36
MnO	1.23	0.00	1.11	0.00	0.00	0.00	0.00	0.00	0.00	0.00	0.00	0.00	0.00
MgO	41.35	49.50	52.64	52.77	18.02	18.35	18.15	18.10	18.01	23.37	22.92	24.41	24.08
NiO	0.00	0.00	0.00	0.00	0.00	0.00	0.00	0.00	0.00	0.00	0.00	0.00	0.00
CaO	0.00	0.00	0.00	0.00	26.29	26.95	27.00	27.22	27.81	13.36	13.60	13.70	13.88
Na_2O	0.00	0.00	0.00	0.00	0.00	0.00	0.00	0.00	0.00	0.00	0.00	0.00	0.00
Total	97.29	94.89	100.27	100.32	99.90	100.21	100.56	100.45	100.79	97.61	97.77	98.37	98.37
Si	4.02	3.97	1.00	1.00	1.96	1.98	1.96	1.95	2.04	7.98	8.01	7.95	7.86
Ti	0.33	0.28	0.00	0.00	0.00	0.00	0.00	0.00	0.00	0.00	0.00	0.00	0.00
Cr	0.00	0.00	0.00	0.00	0.00	0.00	0.00	0.00	0.00	0.00	0.00	0.00	0.00
Al	0.00	0.00	0.00	0.00	0.00	0.00	0.00	0.00	0.00	0.08	0.00	0.00	0.12
Fe^{+3}	0.00	0.00	0.00	0.00	0.00	0.00	0.00	0.00	0.00	0.00	0.00	0.00	0.00
Fe^{+2}	1.50	0.57	0.10	0.12	0.05	0.00	0.03	0.04	0.01	0.22	0.31	0.18	0.15
Mn	0.12	0.00	0.02	0.00	0.00	0.00	0.00	0.00	0.00	0.00	0.00	0.00	0.00
Mg	7.04	8.17	1.88	1.88	0.97	0.98	0.97	0.97	0.98	4.75	4.67	4.93	4.89
Ni	0.00	0.00	0.00	0.00	0.00	0.00	0.00	0.00	0.00	0.00	0.00	0.00	0.00
Ca	0.00	0.00	0.00	0.00	1.02	1.04	1.04	1.05	1.01	1.95	1.99	1.99	2.02
Na	0.00	0.00	0.00	0.00	0.00	0.00	0.00	0.00	0.00	0.00	0.00	0.00	0.00

TABLE 4
Representative SEM-EDS analyses of antigorite

Vein type	Type 2			Type 3		Type 4					
Sample	OF2953	OF2954	OF2957	OF3255	OF3255	OF2831	OF2855	OF2864	OF2945	OF2956	OF3265
Locality	(g)	(g)	(f)	(u)	(u)	(a)	(b)	(d)	(i)	(b)	(r)
Analyses	3.2	1.12	3.5	1.10	1.26	3.5	9.4	1.2	2.9	2.1	2.3
SiO2	41.95	42.48	42.72	42.93	42.61	42.53	42.90	43.24	42.40	42.47	41.51
Cr2O3	0.00	0.00	0.00	0.00	0.00	0.00	0.00	0.00	0.40	0.00	0.00
Al2O3	2.18	2.42	2.34	1.27	1.83	2.71	2.37	1.75	2.68	1.94	2.17
FeO	3.01	3.05	2.56	1.87	1.99	3.07	2.91	1.92	2.55	4.39	5.35
MgO	38.71	39.12	39.23	40.07	39.91	38.80	39.10	40.16	39.11	38.51	36.69
NiO	0.00	0.00	0.00	0.00	0.00	0.00	0.00	0.00	0.00	0.00	0.00
Total	85.85	87.07	86.84	86.14	86.34	87.10	87.28	87.07	87.13	87.31	85.72
Si	2.00	2.00	2.01	2.03	2.01	2.00	2.02	2.03	1.99	2.01	2.01
AlIV	0.00	0.00	0.00	0.00	0.00	0.00	0.00	0.00	0.01	0.00	0.00
AlVI	0.12	0.13	0.13	0.07	0.10	0.15	0.13	0.10	0.14	0.11	0.12
Fe+3	0.00	0.00	0.00	0.00	0.00	0.00	0.00	0.00	0.00	0.00	0.00
Fe+2	0.12	0.12	0.10	0.07	0.08	0.12	0.11	0.08	0.10	0.17	0.22
Mg	2.75	2.75	2.76	2.82	2.81	2.72	2.74	2.80	2.74	2.71	2.65
Cr	0.00	0.00	0.00	0.00	0.00	0.00	0.00	0.00	0.01	0.00	0.00
Ni	0.00	0.00	0.00	0.00	0.00	0.00	0.00	0.00	0.00	0.00	0.00

al. (2004) and Groppo *et al.* (2006) for chrysotile and fibrous antigorite, Rinaudo *et al.* (2004) for tremolite, Huang *et al.* (2000) for diopside, Belluso *et al.* (2007) for carlosturanite and Rosasco and Blaha (1978) for talc.

Antigorite and chrysotile

In both fibrous antigorite and chrysotile the main peaks in the Raman spectrum are related to the symmetric Si-O_b-Si stretching and SiO_4 bending modes, which occur at about 680 and 380 cm^{-1} in antigorite, and 692 and 390 cm^{-1} in chrysotile, respectively (Rinaudo *et al.*, 2003; Groppo *et al.*, 2006). Furthermore, antigorite may also be easily distinguished from chrysotile on the basis of the 1045 cm^{-1} antisymmetric Si-O_b-Si stretching mode (Figs. 9a,c). Two strong peaks at 230 cm^{-1} in antigorite and 235 cm^{-1} in chrysotile are related to the O-H-O vibrational modes. In the OH vibrational region antigorite and chrysotile are also characterized by different micro-Raman spectra. Antigorite shows two main bands at about 3668 and 3698 cm^{-1}, whereas chrysotile shows a major, asymmetric band at about 3684 cm^{-1}, with a tail toward lower frequencies, and a less pronounced peak at about 3704 cm^{-1} (see also Auzende *at al*., 2004) (Figs. 9b,d).

Variations in the chemical composition of chrysotile and antigorite do not significantly influence the position of these main peaks, which are only shifted of 2-3 cm^{-1}. Nevertheless, it had been observed (Groppo *et al.*, 2006) that serpentine minerals with significant Al substituting for Mg in the octahedral layer show a large band in the 900-950 cm^{-1} spectral region, clearly related to the presence of Al in the octahedral sites.

Balangeroite and carlosturanite

Micro-Raman spectra of balangeroite and carlosturanite have been acquired for both fibrous and prismatic varieties and their interpretation is still in progress (see also Belluso *et al*., 2007). Two main peaks appear in the balangeroite spectrum, at 685 and 984 cm^{-1} (Fig. 10a), whereas in the more complex carlosturanite spectrum the main peaks appear at 672, 703 and 776 cm^{-1} (Fig. 10c). In both minerals these peaks are probably related to Si-O-Si stretching modes. In the fibrous varieties of both balangeroite and carlosturanite which are partially replaced by chrysotile, the main peaks of chrysotile (390 and 692 cm^{-1}) may partially overlap those of balangeroite and carlosturanite. For this reason the spectra acquired on the prismatic samples are reported as reference.

Balangeroite and carlosturanite spectra differ from those of associated antigorite and chrysotile also in the OH vibrational region. In particular, balangeroite shows several peaks in the 3500-3700 cm^{-1} frequency range, the strongest peaks being at 3569, 3558 and 3509 cm^{-1} (Fig. 10b). The carlosturanite spectrum is more simple and shows two main peaks at 3585 and 3685 cm^{-1} (Fig. 10d).

Diopside and tremolite

The main peaks in the micro-Raman spectrum of fibrous diopside occur at about 1015 and 670 cm^{-1} and correspond to the symmetric Si-O-Si stretching and O-Si-O bending modes, respectively (Fig. 11c). The Mg-O stretching modes give relatively intense peaks at 142, 327 and 394 cm^{-1} (Huang *et al.*, 2000).

Symmetric and antisymmetric Si-O-Si stretching modes of fibrous tremolite give peaks at about 676, 935 cm^{-1} and 1032, 1062 cm^{-1}, respectively, which are also the strongest peaks (Fig. 11a). O-H-O vibrations produce two other strong peaks at about 225 and 234 cm^{-1} (Rinaudo *et al.*, 2004). In the OH vibrational region tremolite shows only two peaks, the most intense at 3675 cm^{-1}, and the second at 3662 cm^{-1} (Fig. 11b).

Brucite and talc

Brucite shows two main peaks at 281 and 444 cm^{-1} and two peaks at 3644 and 3651 cm^{-1} in the OH-vibrational region (Figs. 11e,f). Talc is characterized by a sharp peak at 197 cm^{-1}; the 365, 678 and 1054 cm^{-1} peaks (Fig. 11d) are related to the symmetric SiO_4 bending, Si-O_b-Si stretching and Si-O_{nb}-Si stretching modes, respectively (Rosasco and Blaha, 1978). In the OH vibrational region the main peak occurs at 3675 cm^{-1}.

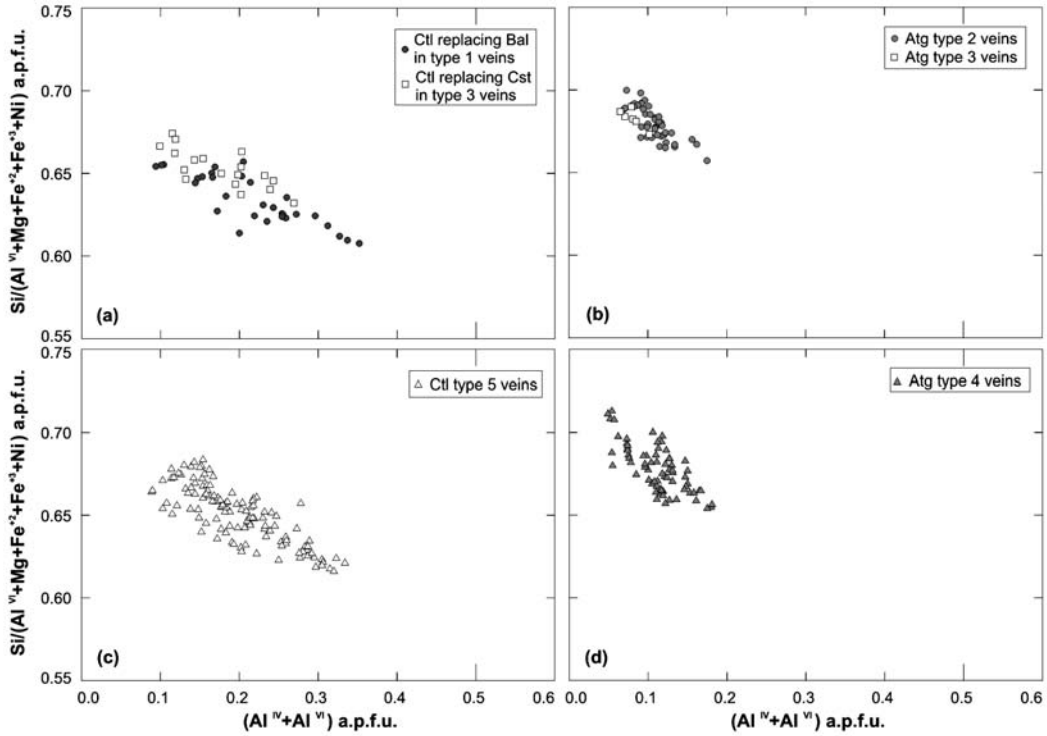

Fig. 7 – Al *vs.* Si/(Σ octahedral cations) diagram for chrysotile occurring in veins of type 1, 3 (a) and 5 (c) and fibrous

TABLE 5
Diagnostic peaks in micro-Raman spectra of fibrous minerals

Antigorite			230		380		680							3668	3698	
Chrysotile			235		390		692								3684	3704
Balangeroite							685		984			3509	3558-3569			
Carlosturanite							672	703-776					3587		3685	
Diopside	142			327	394		670			1015						
Tremolite		224-234					676		935	1032	1062			3662	3675	
Talc	196				365		678							3660	3675	3698
Brucite				281		444								3651		

DISCUSSION: GENETIC CONDITIONS OF METAMORPHIC VEINS OCCURRING IN SERPENTINITES

Veins 1 – Balangeroite + magnetite + Fe-Ni alloys (+ chrysotile)

The balangeroite stability field is still unknown due to the lack of experimental data, but genetic conditions for type 1 veins may be inferred from their mineral assemblages and microstructural relationships with the other vein generations. Relict prismatic balangeroite often includes antigorite flakes, thus suggesting that balangeroite was stable together with antigorite. Fibrous balangeroite is

partially replaced by chrysotile, most probably according to the reaction:

$$Mg_{42}O_6(OH)_{40}(Si_4O_{12})_4 + 12SiO_2 + 8H_2O = 14Mg_3Si_2O_5(OH)_4$$

balangeroite — chrysotile

as suggested by Ferraris *et al.* (1987). The presence of the Fe-Ni alloys awaruite and taenite associated with balangeroite suggests low $f(O_2)$ during its development. A further constraint is that metamorphic olivine and diopside belonging to the peak paragenesis statically overgrow fibrous balangeroite (Fig. 3d). The above observations suggest that type 1 veins formed during prograde high pressure metamorphism within the antigorite stability field and under reducing conditions.

Veins 2 – Diopside + Ti-clinohumite + olivine + Mg-chlorite + antigorite + magnetite

Though Ti-clinohumite has a wide stability field (Rahn and Bucher, 1998), the assemblage diopside + Ti-clinohumite + olivine + Mg-chlorite + antigorite + magnetite of type 2 veins in the Alps is typical of eclogite-facies metamorphism, as observed by Compagnoni *et al.* (1980) and Scambelluri *et al.* (1991) for the serpentinites from the Lanzo and Voltri Massifs, respectively. The stability field of the peak assemblage is limited towards lower temperatures by the reaction

$$Atg + Brc = Ol + H_2O \quad (1),$$

and towards higher temperatures by the reaction

$$Atg = Ol + Tlc + H_2O \quad (2).$$

In a serpentinite sample from the Monviso metaophiolite (Val Pellice), ilmenite and antigorite (+ magnesite) have been observed as the breakdown products of Ti-clinohumite (Fig. 3h), according to the reaction suggested by Trommsdorff and Evans (1980):

$$17\,Ti\text{-}cl + 107\,H_2O + 80\,CO_2 = 4\,Atg + 80\,Mag + 17\,Ilm \quad (3).$$

This reaction is entirely inside the stability field of antigorite, thus suggesting that the retrograde *P-T* path, necessary for the development of ilmenite + antigorite + magnesite at the expense of Ti-clinohumite must have occurred within the antigorite stability field, i.e. at $T<650$°C. The peak conditions inferred from the associated metabasite (550-550°C, 1.5-1.6 GPa – Pognante, 1991) and metagabbro (550-620°C, 2.0 GPa – Pelletier and Müntener, 2006) from the Internal Piemonte Zone are in good agreement with the stability field of the peak paragenesis.

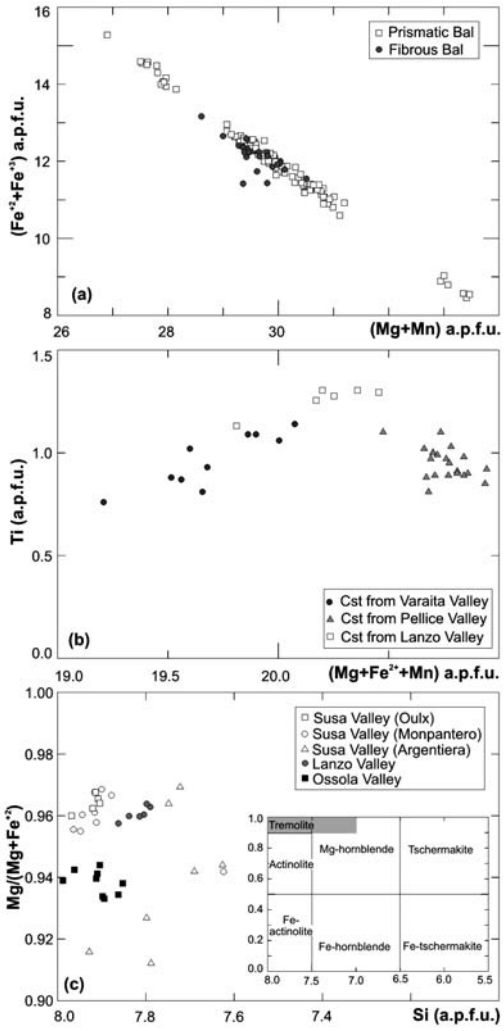

Fig. 8 – (a) (Mg+Mn) *vs.* (Fe^{+2}+Fe^{+3}) diagram for prismatic and fibrous balangeroite of veins of type 1. (b) (Mg+Fe^{+2}+Mn) *vs.* Ti diagram for prismatic and fibrous carlosturanite of veins of type 3. (c) Si *vs.* Mg/(Mg+Fe^{+2}) diagram for tremolite of veins of type 6. In the inset the classification diagram of Ca-amphibole (Leake *et al.*, 1998) is reported.

Veins 3 – Carlosturanite + antigorite + diopside + garnet (+ chrysotile + brucite)

As for balangeroite, the stability field of carlosturanite is still unknown, but possible genetic conditions for type 3 veins may be inferred

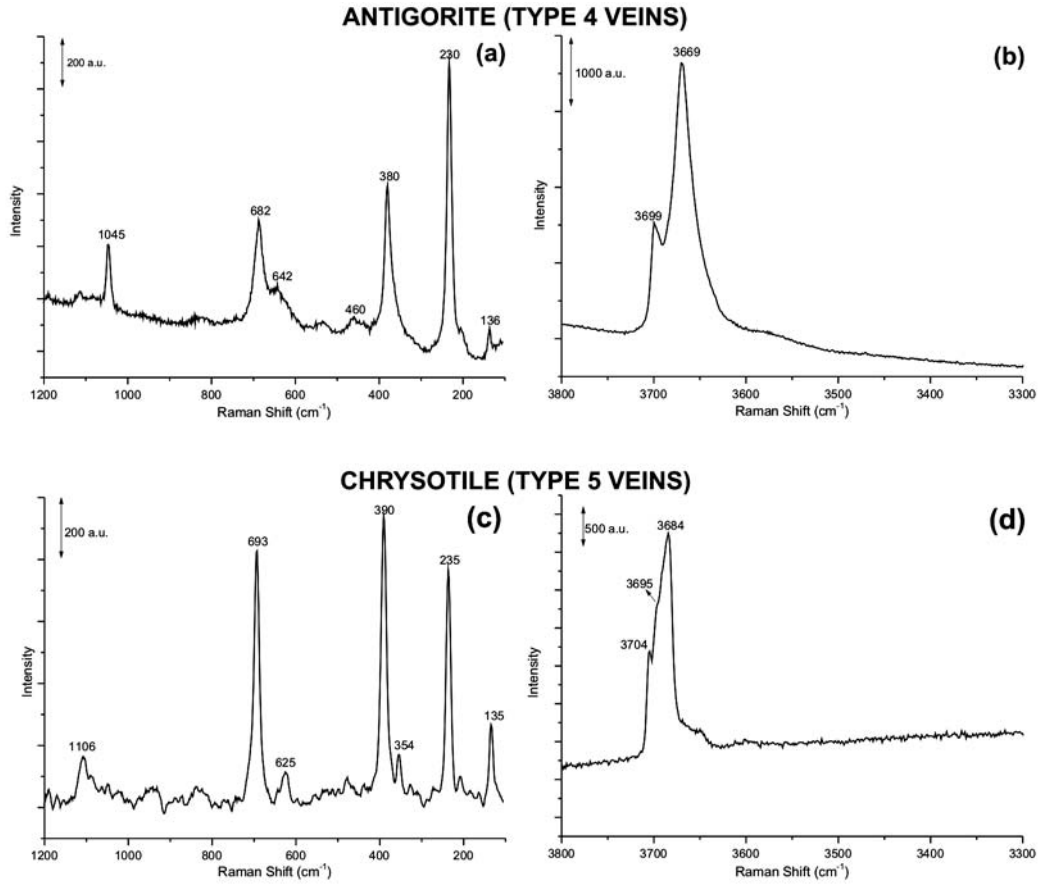

Fig. 9 – μ-Raman spectra (green laser) of fibrous antigorite and chrysotile from veins of type 4 (a, b) and 5 (c,d) in the frequency ranges 100-1200 cm^{-1} and 3300-3800 cm^{-1}, respectively.

from both their paragenesis and microstructural relationships with the other vein generations. As suggested by the vein assemblage, carlosturanite developed in the diopside + antigorite stability field, and is replaced by the chrysotile + brucite assemblage (Mellini *et al.*, 1985; Baronnet and Belluso, 2002). Furthermore, the discovery of relict Ti-clinohumite partially replaced by carlosturanite (Figs. 4g,h) is a clear evidence that type 3 veins developed at the expense of the high pressure peak paragenesis. Therefore, it can be concluded that type 3 veins formed within the antigorite stability field during the early retrograde portion of the exhumation *P-T* path.

Veins 4 – Antigorite + diopside

Microstructural relationships with the other vein generations suggest that fibrous antigorite has formed during the decompressional evolution of Piemonte Zone serpentinites, later than the carlosturanite-bearing type 3 veins, but prior to the development of the chrysotile asbestos veins (Groppo and Compagnoni, 2007). Fibrous antigorite veins, in fact, are often crosscut by slip and/or cross fibre chrysotile veins, which probably formed during later vein opening events in a very shallow environment.

The antigorite *a* parameter of 43.0-43.8 Å, determined by TEM-SAED, corresponds to $m = 17$

on the base of the data from Mellini *et al.* (1987). Taking into consideration the results of Mellini *et al.* (1987) and Wunder *et al.* (2001) it may be suggested that the studied fibrous antigorite formed at $T \approx 350$-450°C. This suggestion, however, must be considered with care, since the *m*-value of antigorite is not only dependent on *P* and *T* but also on additional factors, such as mineral assemblage, water activity, and bulk chemical composition, especially the Al and Fe contents (Wunder *et al.*, 2001).

The fibrous habit of antigorite may be explained as the result of two different mechanisms, i.e. the crack-seal and the dissolution-precipitation creep. These processes are equally able to explain the banded structure of the studied veins and are compatible with the estimated *P*-*T* conditions of formation (Groppo and Compagnoni, 2007). A third possibility, i.e. the epitaxial replacement of former chrysotile veins (Laurent and Hébert, 1979; Baronnet *et al.*, 1994; Baronnet and Devouard, 1996), also exists. However, this mechanism can be excluded for the type 4 veins, since microstructural observations clearly show that fibrous antigorite veins developed during the exhumation history of the serpentinites, earlier than the chrysotile vein formation. The antigorite replacement of chrysotile implies a prograde evolution, which

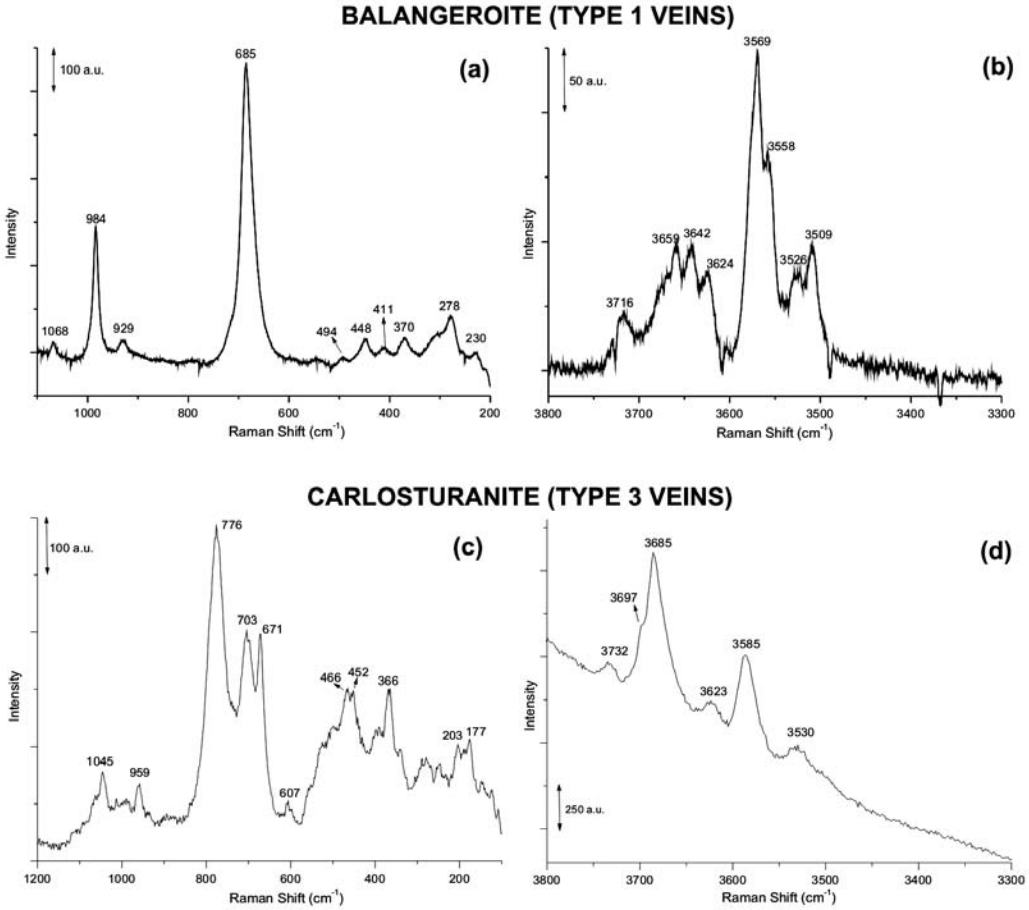

Fig. 10 – **μ-Raman spectra (a,b: red laser; c,d: green laser) of prismatic balangeroite and carlosturanite from veins of type 1** and 3, respectively, in the frequency ranges 200-1100 cm^{-1} (a), 100-1200 cm^{-1} (c), and 3300-3800 cm^{-1} (b,d).

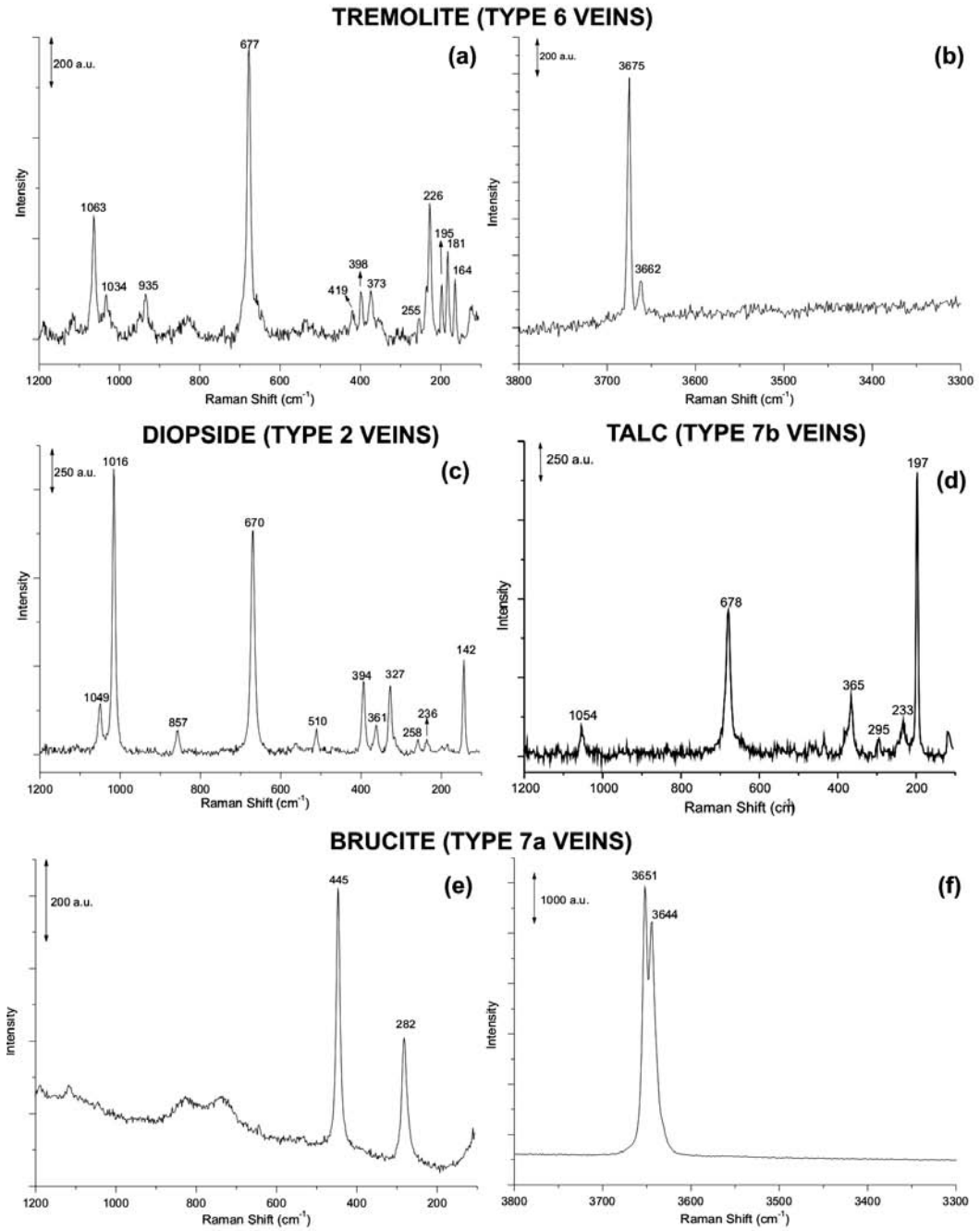

Fig. 11 – µ-Raman spectra (green laser) of fibrous tremolite (a,b), diopside (c), talc (d) and brucite (e,f) from veins of type 6, 2, 7b and 7a, respectively, in the frequency ranges 100-1200 cm^{-1} (a, c,d,e) and 3300-3800 cm^{-1} (b,f).

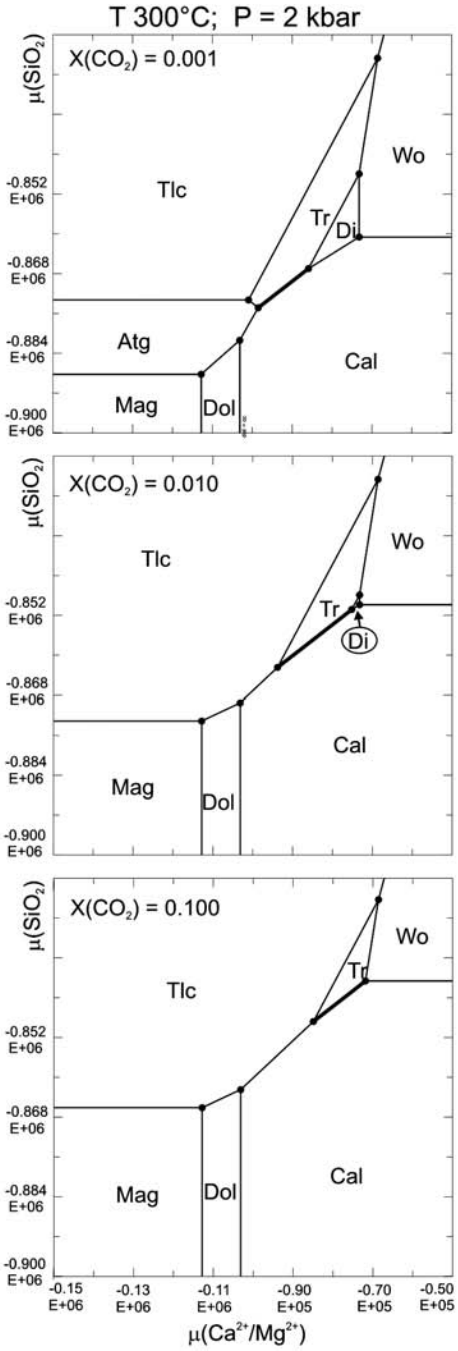

Fig. 12 – $\mu(Ca^{2+}/Mg^{2+})$ *vs.* $\mu(SiO_2)$ diagrams in the CMSH system for different $X(CO_2)$ values. The tremolite (Tr) + is exactly the opposite of the observed *P-T* path. Thus, the fibrous habit of antigorite is not due to the replacement of a former fibrous mineral, but to the mechanisms of vein formation by crack-seal or dissolution-precipitation creep.

Veins 5 – Chrysotile

Microstructural relationships with the other vein generations suggest that type 5 veins formed late in the serpentinite evolution, just before the tremolite-bearing type 6 veins. Most likely the chrysotile veins formed at very shallow levels (Compagnoni *et al.*, 1980; Pognante *et al.*, 1985) during the brittle deformation of serpentinites, since chrysotile grows as vein-filling cross- and slip-type fibres. As suggested by Evans (2004), the growth of either slip or cross-fibre chrysotile is closely related to the extension processes. Porosity together with the presence of a fluid phase oversaturated in Mg and Si are indicated as the key factors controlling the growth of chrysotile (Evans, 2004).

Veins 6 – Tremolite ± calcite

Microstructural observations clearly show that the tremolite-bearing veins are the last generation of metamorphic veins in the serpentinites of both External and Internal Piemonte Zone, since they crosscut both the antigorite type 4 and the chrysotile type 5 veins. The occurrence of calcite suggests that the tremolite development is controlled by the presence of CO_2 in the fluid phase and by the bulk chemical composition. The relative stability of tremolite + calcite (Tr + Cal) with respect to diopside + calcite (Di + Cal) has been investigated by means of the $\mu(Ca^{2+}/Mg^{2+})$ *vs.* μSiO_2 diagrams at different $X(CO_2)$ contents in the fluid phase (Fig. 12). These diagrams show that at very low $X(CO_2)$ the Tr + Cal assemblage is favoured by lower $\mu(Ca^{2+}/Mg^{2+})$ and μSiO_2, whereas at higher $X(CO_2)$ [$X(CO_2)$>0.01] the assemblage Di + Cal is not stable. At increasing $X(CO_2)$ values the paragenesis talc + calcite becomes progressively more stable.

Other vein types : brucite + magnetite and talc + calcite

Microstructural observations suggest that both brucite + magnetite and talc + calcite veins are relatively late in the serpentinite evolution. Their formation is most likely due to the local occurrence of special conditions. As for the tremolite-bearing veins, the development of talc + calcite assemblage is favoured by relatively high $X(CO_2)$ values in the fluid phase (Fig.12).

CONCLUSIONS

On the basis of the reported petrological and microstructural data, it may be concluded that:

(i) Seven different vein generations, developed at different *P-T-X* conditions, have been recognised in the serpentinites from the Piemonte Zone. The first vein generation (balangeroite + magnetite + FeNi-alloys) formed during the serpentinite prograde evolution, whereas the second vein generation (diopside + Ti-clinohumite + olivine + antigorite + Mg-chlorite) is related to the high pressure peak metamorphic event. All the others vein generations developed during the retrograde serpentinite evolution, at different *P-T* conditions, moderate for types 3 and 4 and low or very low for types 5, 6 and 7.

(ii) Serpentinites are generally very fine grained and recrystallize very easily, obliterating the older microstructural relationships. On the contrary, the metamorphic veins crosscutting serpentinites often preserve mineral assemblages which are indicative of different stages of the *P-T* evolution. Metamorphic veins are then much more informative than the host rock in reconstructing the serpentinite evolution.

(iii) Micro-Raman spectroscopy may be applied routinely as a successful technique complementary to optical and electron microscopy for a quick and reliable identification of fibrous minerals occurring in serpentinites, since the laser resolution is comparable to the fibre cross dimension.

ACKNOWLEDGEMENTS

This work is part of a multidisciplinary research project entitled “Asbestos Hazard in the western Alps”, supported by Regione Piemonte (Italy) and coordinated by the Interdepartmental Centre “Giovanni Scansetti” for Studies on Asbestos and Other Toxic Particulates at the University of Turin. We are grateful to A.-M. Boullier and B.W. Evans for careful and constructive reviews and to G. Ferraris for useful discussion and suggestions. The micro-Raman data have been obtained with the equipment acquired by the Interdepartmental Centre “G. Scansetti” for Studies on Asbestos and Other Toxic Particulates with a grant from Compagnia di San Paolo, Torino.

REFERENCES

AGARD P., GOFFÉ B., TOURET L.R. and VIDAL O. (2000) – *Retrograde mineral and fluid evolution in high pressure metapelites (Schistes Lustrés Unit, western Alps)*. Contrib. Mineral. Petrol., **140**, 296-315.

AGARD P., JOLIVET L., and GOFFÉ B. (2001) – *Tectonometamorphic evolution of the Schistes Lustrés complex: implications for the exhumation of HP and UHP rocks in the western Alps*. Bull. Soc. Geol. France, **172**, 617-636.

ALBERICO A., BELLUSO E., COMPAGNONI R. and FERRARIS G. (1997) – *Amianti ed altri minerali asbestiformi sul territorio piemontese*. In**:** Giornata di Studio su: Il rischio amianto legato alle attività estrattive e alla bonifica di siti industriali dismessi. Torino, 20 maggio 1997, Regione Piemonte e Associazione Georisorse e Ambiente, Torino, Italy, 97-102.

ALBINO G.V. (1995) – *Iron- and aluminium-rich serpentine and chlorite from the Boundary Ultramafic Complex, Cape Smith Belt, New Quebec*. Can. Mineral., **33**, 559-568.

ANDREANI M., BARONNET A., BOULLIER A.-M. and GRATIER, J.-P. (2004) – *A microstructural study of a «crack-seal» type serpentine vein using SEM and TEM techniques*. Eur. J. Mineral., **16**, 585-595.

AUZENDE A.-L., DANIEL I., REYNARD B., LEMAIRE C. and GUILLOT F. (2004) – *High pressure behaviour of serpentine minerals: a Raman spectroscopy study*. Phys. Chem. Minerals, **31**, 269-277.

BARNICOAT A.C. and FRY N. (1986) – *High-pressure metamorphism of the Zermatt-Saas ophiolite zone, Switzerland*. J. Geol. Soc. London, **143**, 607-618.

BARNICOAT A.C. and FRY N. (1989) – *Eoalpine high-pressure metamorphism in the Piemonte zone of the Alps: Southwest Switzerland and northwest Italy*. In: DALY J.S., CLIFF R.A. and YARDLEY B.W.D. (Eds.) – Evolution of Metamorphic Belts. Geol. Soc. London, Spec. Publ., **43**, 539-544.

BARONNET A. and BELLUSO E. (2002) – *Microstructures of the silicates: key information about mineral reactions and a link with the Earth and materials sciences*. Mineral. Mag., **66**, 709-732.

BARONNET A. and DEVOUARD B. (1996) – *Topology and crystal growth of natural chrysotile and polygonal serpentine*. J. Cryst. Growth, **166**, 952-960.

BARONNET A., MELLINI M. and DEVOUARD B. (1994) – *Sectors in polygonal serpentine, a model based on dislocations*. Phys. Chem. Min., **21**, 330-343.

BELLUSO E. and FERRARIS G. (1991) – *New data on balangeroite and carlosturanite from alpine serpentinites*. Eur. J. Mineral., **3**, 559-566.

BELLUSO E., FORNERO E., ALBERTAZZI G., CAIRO S. and RINAUDO C. (2007) – *Using the micro-Raman spectroscopy to distinguish carlosturanite from the serpentine minerals.* Can. Mineral. (in press).

BENCE A.E. and ALBEE A.L. (1968) – *Empirical correction factors for the electron microanalysis of silicates and oxides*. J. Geol., **76**, 382-402.

BODINIER J.L. (1988) – *Geochemistry and petrogenesis of the Lanzo peridotite body, western Alps*. Tectonophysics, **149**, 67-88.

BOUDIER F. (1971) – *Minéraux serpentineux extraits de péridotites serpentinisées des Alpes Occidentales*. Contrib. Mineral. Petrol., **33**, 331-345.

BOUDIER F. (1976) – *Le massif lherzolitique de Lanzo (Alpes piémontaise). Etude structurale et pétrologique*. Thèse de doctorat d'état, University of Nantes, 175 pp.

BROMILEY G.D. and PAWLEY A.R. (2003) – *The stability of antigorite in the system MgO-SiO_2-H_2O (MSH) and MgO-Al_2O_3-SiO_2-H_2O (MASH): The effects of Al^{3+} substitution on high pressure stability*. Am. Mineral., **88**, 99-108.

BUCHER K., FAZIS Y., DE CAPITANI C., and GRAPES R. (2005) – *Blueschists, eclogites, and decompression assemblages of the Zermatt-Saas ophiolite: High-pressure metamorphism of subducted Tethys lithosphere*. Am. Mineral., **90**, 821-835.

CARTWRIGHT I. and BARNICOAT A.C. (2002) – *Petrology, geochronology, and tectonics of shear zones in the Zermatt-Saas and Combin zones of the western Alps*. J. Metam. Geol., **20**, 263-281.

CASTELLI D., ROLFO F. and ROSSETTI P. (1995) – *Petrology of ore-bearing rodingite veins from the Balangero asbestos mine (western Alps).* In: LOMBARDO B. (Ed.) Studies on metamorphic rocks and minerals in the western Alps. A Volume in Memory of Ugo Pognante. Boll. Mus. Reg. Sci. Nat. (Torino, Italy), **13**, 153-189.

COMPAGNONI R., FERRARIS G. and FIORA L. (1983) – *Balangeroite, a new fibrous silicate related to gageite from Balangero, Italy*. Am. Mineral., **6**, 214-219.

COMPAGNONI R., FERRARIS G. and MELLINI M. (1985) – *Carlosturanite, a new asbestiform rock-forming silicate from Val Varaita, Italy*. Am. Mineral., **70**, 767-772.

COMPAGNONI R., SANDRONE R. and ZUCCHETTI S. (1980) – *Some remarks on the asbestos occurrences in the western Alps with special reference to the chrysotile asbestos deposit of Balangero (Valle di Lanzo, Piemonte, Italy).* Fourth Conference on Asbestos, Torino, 20-30 May 1980, Preprint, **I**, 49-71.

DERIU A., FERRARIS G. and BELLUSO E. (1994) – *^{57}Fe Mössbauer study of the asbestiform silicates balangeroite and carlosturanite*. Phys. Chem. Min., **21**, 222-227.

DEWEY J.F., HELMA M.L., TURCO E., HUTTON D.H.W. and KNOTT S.D. (1989) – *Kinematics of the western Mediterranean*. In: (COWARD M.P., DIETRICH D. & PARK R.G. (Eds.), Alpine Tectonics, Geol. Soc. London Spec. Publ., **45**, 265–283.

DUNGAN M.A. (1979) – *Bastite pseudomorphs after orthopyroxene, clinopyroxene and tremolite*. Can. Mineral., **17**, 729-740.

ECKSTRAND O.R. (1975) – *The Dumont serpentinite: a model for control of nickeliferous opaque mineral assemblage by alteration reactions in ultramafic rocks*. Econ. Geol., **70**, 183-201.

EVANS B.W. (2004) – *The serpentinite multisystem revisited: chrysotile is metastable*. Int.. Geol. Rev., **46**, 479-506.

EVANS B.W., JOHANNES W., OTERDOOM H. and TROMMSDORFF V. (1976) – *Stability of chrysotile and antigorite in the serpentinite multisystem*. Schweiz. Mineral. Petrogr. Mitt., **56**, 79-93.

FERRARIS G., MELLINI M. and MERLINO S. (1987) – *Electron-diffraction and electron-microscopy study of balangeroite and gageite: crystal structures, polytypism and fiber texture*. Am. Mineral., **72**, 382-391.

FROST B.R. (1985) – *On the stability of sulphides, oxides and native metals in serpentinite*. J. Petrol., **26**, 31-63.

GROPPO C. and COMPAGNONI R. (2007) – *Ubiquitous fibrous antigorite veins from the Lanzo Ultramafic Massif, Internal western Alps: characterization and genetic conditions*. Per. Mineral., **76**, 169-181.

GROPPO C., RINAUDO C., CAIRO S., GASTALDI D. and COMPAGNONI R. (2006) – *Raman Spectroscopy as a rapid method for the identification of serpentine minerals from serpentinized ultramafics*. Eur. J.

Mineral., **18**, 319-329.

GROPPO C., TOMATIS M., TURCI F., GAZZANO E., GHIGO D., COMPAGNONI R. and FUBINI B. (2005) – *Potential toxicity of non-regulated asbestiform minerals: balangeroite from western Alps. Part 1, identification and characterization*. J. Toxic. Environ. Health, **68**, 1-19.

HEY M.H. (1954) – *A new review of the chlorites*. Mineral. Mag., **30**, 277–292.

HUANG E., CHEN C.H., HUANG T., LIN E.H. and XU J.A. (2000) – *Raman spectroscopic characteristics of Mg-Fe-Ca pyroxenes*. Am. Mineral., **85**, 473-479.

KOLITSCH U., BELLUSO E., GULA A. AND FERRARIS G. (2003) – *The crystal structure of an apparently new magnesium silicate mineral: a polytype of carlosturanite?* Mitt. Österr. Miner. Ges., **148**, 194-195.

KUNZE G. (1961) – *Antigorit. Struktur theoretische Grundlagen und ihre praktische Bedeutung für die weitere Serpentin-Forschung*. Fortschr. Mineral. **39**, 206-324.

LAURENT R. and HEBERT Y. (1979) – *Paragenesis of serpentine assemblages in harzburgite tectonite and dunite cumulate from the Quebec Appalachians*. Can. Mineral., **17**, 857- 869.

LEAKE B.E., WOOLLEY A.R., ARPS C.E.S., BIRCH W.D., GILBERT M.C., GRICE J.D., HAWTHORNE F.C., KATO A., MANDARIN, J.A., MARESCH W.V., NIKEL E.H., ROCK N.M.S., SCHUMACHER J.C., SMITH D.C., STEPHENSON N.C.N., UNGARETTI L. WHITTAKER E.J.W. and YOUZHI G. (1997) – *Nomenclature of amphiboles: Report of the Subcommittee on Amphiboles of the International Mineralogical Association, Commission on New Minerals and Mineral Names*. Am. Mineral., **82**, 1019-1037.

LEMOINE M. and TRICART P. (1986) – *Les Schistes Lustrés piémontais des Alpes Occidentales: approche stratigraphique, structurale et sédimentologique*. Ecl. Geol. Helv., **79**, 271-293.

LI X-P., RAHN M.and BUCHER K. (2004) – *Serpentinites of the Zermatt-Saas ophiolite complex and their texture evolution*. J. Metam. Geol., **22**, 159-177.

MELLINI M. (1986) – *Chrysotile and polygonal serpentine from the Balangero serpentinite*. Mineral. Mag., **50**, 301-305.

MELLINI M. and ZUSSMAN J. (1986) – *Carlosturanite (not "picrolite") from Taberg, Sweden*. Mineral. Mag., **50**, 675-679.

MELLINI M., FERRARIS G. and COMPAGNONI R. (1985) – *Carlosturanite: HRTEM evidence of a polysomatic series including serpentine*. Am. Mineral., **70**, 773-781.

MELLINI M., TROMMSDORFF V. and COMPAGNONI R. (1987) – *Antigorite polysomatism: behavior during progressive metamorphism*. Contrib. Mineral. Petrol., **97**, 147-155.

MÜNTENER O., PETTKE T., DESMURS L., MEIER M. and SCHALTEGGER U. (2004) – *Refertilization of mantle peridotite in embryonic ocean basins: trace element and Nd isotopic evidence and implications for crust-mantle relationship*. Earth Planet. Sci. Lett., **221**, 293-308.

NICOLAS A. (1966) – *Etude pétrochimique des roches vertes et de leurs minéraux entre Dora Maira et Grand Paradis (Alpes piémontaises); le complexe ophiolite-schistes lustrés*. Thèse, Fac. Sc. Nantes, 299 pp.

OBERHÄNSLI R., GOFFÉ B. and BOUSQUET R. (1995) – *Record of a HP-LT metamorphic evolution in the Valais Zone*. In: B. Lombardo (Ed.) Studies on metamorphic rocks and minerals of the western Alps. A Volume in Memory of Ugo Pognante. Boll. Mus. Reg. Sc. Nat. (Torino, Italy) Suppl., **13**, 221-239.

PELLETIER L. and MÜNTENER O. (2006) – *High pressure metamorphism of the Lanzo peridotite and its oceanic cover, and some consequences for the Sesia-Lanzo zone (northwestern Italian Alps)*. Lithos, **90**, 111–130.

PICCARDO G.B., MÜNTENER O., ZANETTI A. and PETTKE T. (2004a) – *Ophiolitic peridotites of the Alpine-Apennine system: mantle processes and geodynamic relevance*. Int.. Geol. Rev., **46**, 1119–1159.

PICCARDO G.B., MÜNTENER O., ZANETTI A., ROMAIRONE A., BRUZZONE S., POGGI E. and SPAGNOLO G. (2004b) – *The Lanzo south peridotite: melt/peridotite interaction in the mantle lithosphere of the Jurassic ligurian Tethys*. Ofioliti, **29**, 63-74.

POGNANTE U. (1991) – *Petrological constraints on the eclogite and blueschist-facies metamorphism and P-T-t path in the western Alps*. J. Metam. Geol. **9**, 5-17.

POGNANTE U., RÖSLI U. and TOSCANI L. (1985) – *Petrology of ultramafic and mafic rocks from the Lanzo peridotite body (western Alps)*. Lithos, **18**, 201-214.

POLINO R., DAL PIAZ G.V. and GOSSO G. (1990) – *Tectonic erosion at the Adria margin and accretionary processes for the Cretaceous orogeny in the Alps*. Mém. Soc. Géol. France, **156**, 345–367.

RAHN, M.K. and BUCHER, K. (1998) – *Titanian clinohumite formation in the Zermatt-Saas ophiolites, Central Alps*. Mineral. Petrol., **64**, 1-13.

RAMDOHR P. (1967) – *A widespread mineral association connected with serpentinization*. N. Jb. Miner. Abh., **107**, 241-265.

RAMPONE E. and PICCARDO G.B. (2000) – *The ophiolite-oceanic lithosphere analogue: new insights from the Northern Apennines (Italy)*. In: DILEK Y., MOORES E.M., ELTHON D.and NICOLAS A., (Eds.) Ophiolites and oceanic crust: new insights from field studies and the oceanic drilling program. Geol. Soc. Am. Special Paper, Boulder, Colorado, **349**, 21-34.

REINECKE, T. (1991) – *Very-high-pressure metamorphism and uplift of coesite-bearing metasediments from the Zermatt-Saas zone western Alps*. Eur. J. Min., **3**, 7-17.

REINECKE, T. (1995) – *Ultrahigh and high-pressure metamorphic rocks of the Zermatt-Saas zone, western Alps: Records of burial and exhumation paths*. In: SCHREYER W., RUMMEL F. and STICKHERT B., (Eds.) - High-Pressure Metamorphism in Nature and Experiment. Abstr. Vol. Int. COB. Bochumer Geol. U. Geotech. Arb. **44**, 152-157.

RINAUDO C., BELLUSO E. and GASTALDI D. (2004) – *Assessment of the use of Raman spectroscopy for the determination of amphibole asbestos.* Mineral. Mag., **68**, 455-465.

RINAUDO C., GASTALDI D. and BELLUSO E. (2003) – *Characterization of chrysotile, antigorite and lizardite by FT-Raman spectroscopy*. Can. Mineral., **41**, 883-890.

RIORDON P.H. (1955) – *The genesis of asbestos in ultrabasic rocks*. Econ. Geol., **50**, 67-83.

ROSASCO G.J. and BLAHA J.J. (1978) – *Raman Microprobe spectra and vibrational mode assignments of talc*. Appl. Spectroscopy, **34**, 140-144.

ROSSETTI P. and ZUCCHETTI S. (1988a) – *Early-alpine ore paragenesis in the serpentinites from the Balangero asbestos mine and Lanzo Massif (Internal western Alps)*. Rend. Soc. It. Mineral. Petrol., **43**, 139-149.

ROSSETTI P. and ZUCCHETTI S. (1988b) – *Occurrence of native iron, Fe-Co and Ni-Fe alloys in the serpentinite from the Balangero asbestos mine (Western Italian Alps)*. Ofioliti, **13**, 43-56.

ROSSETTI P., SANDRONE R. and ZUCCHETTI S. (1987) – *Mineralogical constraints on the recovery of nickel from an ophiolitic ultramafic in the Balangero asbestos mine (Italy)*. In: Troodos'87 Ophiolites and Oceanic Lithosphere Symp., Cyprus Geol. Surv., Nicosia, Abs. 157.

SCAMBELLURI M., HOOGERDUIJN STRATING E.-H., PICCARDO G.B., VISSERS R.L.M. and RAMPONE E. (1991) – *Alpine olivine and titanian clinohumite-bearing assemblages in the Erro-Tobbio peridotite (Voltri Massif, NW Italy)*. J. Metam. Geol., **9**, 79-91.

TROMMSDORFF, V. and EVANS, B.W. (1980) – *Titanian hydroxyl-clinohumite: Formation and breakdown in antigorite rocks (Malenco, Italy)*. Contrib. Mineral. Petrol., **72**, 229-242.

VITI C. (1995) – *I serpentini dell'Isola d'Elba*. PhD Thesis, Università degli Studi di Siena, 59 pp.

VITI C. and MELLINI M. (1996) – *Vein antigorites from Elba Island, Italy*. Eur. J. Mineral., **8**, 423-434.

WICKS F. J. and O'HANLEY D.S. (1988) – *Serpentine minerals: structures and petrology*. In: BAILEY S. (Ed.) - Hydrous phyllosilicates. Reviews in Mineralogy**, 19**, Mineral.Soc. Am, Washington DC, 91-167.

WICKS F.J. and PLANT A.G. (1979) – *Electron-microprobe and X-ray-microbeam studies of serpentine textures*. Can. Mineral., **17**, 785-830.

WICKS F.J. and WHITTAKER E.J.W. (1975) – *A reappraisal of the structures of the serpentine minerals*. Can. Mineral., **13**, 227-243.

WICKS F.J. and WHITTAKER E.J.W. (1977) – *Serpentine textures and serpentinization*. Can. Mineral., **15**, 449-488.

WICKS F. J., WHITTAKER E.J.W. and ZUSSMAN J. (1977) – *An idealized model for serpentine textures after olivine*. Can. Mineral., **15**, 446-458.

WUNDER B., WIRTH R. and GOTTSCHALK M. (2001) – *Antigorite: pressure and temperature dependence of polysomatism and water content*. Eur. J. Mineral., **13**, 485-495.